U.S. DEPARTMENT OF COMMERCE
National Technical Information Service
PB80-128689

Calcium Sulfite Crystal Sizing Studies

Radian Corp, Austin, TX

Prepared for

Industrial Environmental Research Lab, Research Triangle Park, NC

Aug 79

TECHNICAL REPORT DATA
(Please read Instructions on the reverse before completing)

1. REPORT NO. EPA-600/7-79-192	2.	3. RECIPIENT'S ACCESSION NO. PB 80 128689
4. TITLE AND SUBTITLE Calcium Sulfite Crystal Sizing Studies		5. REPORT DATE August 1979 6. PERFORMING ORGANIZATION CODE
7. AUTHOR(S) Larry O. Edwards		8. PERFORMING ORGANIZATION REPORT NO.
9. PERFORMING ORGANIZATION NAME AND ADDRESS Radian Corporation 8500 Shoal Creek Boulevard Austin, Texas 78766		10. PROGRAM ELEMENT NO. EHE624 11. CONTRACT/GRANT NO. 68-02-2608, Task 30
12. SPONSORING AGENCY NAME AND ADDRESS EPA, Office of Research and Development Industrial Environmental Research Laboratory Research Triangle Park, NC 27711		13. TYPE OF REPORT AND PERIOD COVERED Task Final; Through 12/78 14. SPONSORING AGENCY CODE EPA/600/13

15. SUPPLEMENTARY NOTES IERL-RTP project officer is Robert H. Borgwardt, Mail Drop 65, 919/541-2336.

16. ABSTRACT The report describes a reliable experimental method that can be used routinely to determine the crystal size distribution function, a measure that is required for a mathematical representation of the nucleation and growth processes involved in the settling, dewatering, and disposal of calcium sulfite sludge from lime/limestone or dual alkali scrubbers, a major problem associated with coal burning. (A recent EPA report presented a mathematical description of the SO2 scrubbing process, but found discrepancies in the particle size distribution function when measured by different techniques.) Optical and instrumental crystal sizing methods were compared and the merits of each discussed; Coulter counting is recommended. The two primary crystal forms, platelets and granules, were shown to be related: granules are clusters of platelets. Platelets, the preferred shape, form only in slow growth conditions and require seeding. Particle clusters complicate the crystal definition and counting processes. The crystal size distribution was shown to be the sum of several exponential population curves. Fly ash, if present, will dominate counts for particles smaller than 1 micron.

17. KEY WORDS AND DOCUMENT ANALYSIS

a. DESCRIPTORS		b. IDENTIFIERS/OPEN ENDED TERMS	c. COSATI Field/Group
Pollution	Mathematical Models	Pollution Control	13B
Calcium Oxides		Stationary Sources	07B 12A
Sulfites	Nucleation	Calcium Sulfite	
Sludge	Crystal Growth	Dual Alkali System	07A
Crystals	Scrubbers	Instrumental Measurement	20B
Measurement	Calcium Carbonates		14B
Alkalies	Sulfur Oxides		07D

18. DISTRIBUTION STATEMENT Release to Public	19. SECURITY CLASS *(This Report)* Unclassified	21. NO. OF PAGES 97
	20. SECURITY CLASS *(This page)* Unclassified	22. PRICE A05 - A01

EPA Form 2220-1 (9-73)

PB80-124689

United States
Environmental Protection
Agency

Industrial Environmental Research
Laboratory
Research Triangle Park NC 27711

EPA-600/7-79-192
August 1979

EPA

Calcium Sulfite Crystal Sizing Studies

Interagency Energy/Environment R&D Program Report

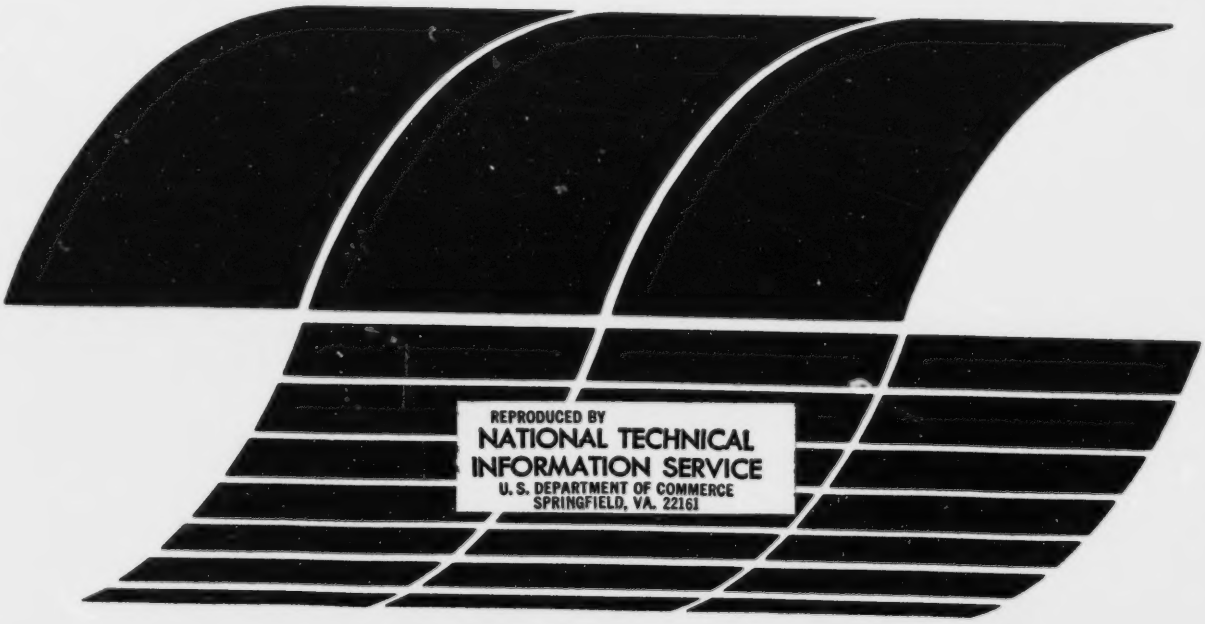

REPRODUCED BY
NATIONAL TECHNICAL
INFORMATION SERVICE
U. S. DEPARTMENT OF COMMERCE
SPRINGFIELD, VA. 22161

RESEARCH REPORTING SERIES

Research reports of the Office of Research and Development, U.S. Environmental Protection Agency, have been grouped into nine series. These nine broad categories were established to facilitate further development and application of environmental technology. Elimination of traditional grouping was consciously planned to foster technology transfer and a maximum interface in related fields. The nine series are:

1. Environmental Health Effects Research
2. Environmental Protection Technology
3. Ecological Research
4. Environmental Monitoring
5. Socioeconomic Environmental Studies
6. Scientific and Technical Assessment Reports (STAR)
7. Interagency Energy-Environment Research and Development
8. "Special" Reports
9. Miscellaneous Reports

This report has been assigned to the INTERAGENCY ENERGY-ENVIRONMENT RESEARCH AND DEVELOPMENT series. Reports in this series result from the effort funded under the 17-agency Federal Energy/Environment Research and Development Program. These studies relate to EPA's mission to protect the public health and welfare from adverse effects of pollutants associated with energy systems. The goal of the Program is to assure the rapid development of domestic energy supplies in an environmentally-compatible manner by providing the necessary environmental data and control technology. Investigations include analyses of the transport of energy-related pollutants and their health and ecological effects; assessments of, and development of, control technologies for energy systems; and integrated assessments of a wide range of energy-related environmental issues.

EPA REVIEW NOTICE

This report has been reviewed by the participating Federal Agencies, and approved for publication. Approval does not signify that the contents necessarily reflect the views and policies of the Government, nor does mention of trade names or commercial products constitute endorsement or recommendation for use.

This document is available to the public through the National Technical Information Service, Springfield, Virginia 22161.

EPA-600/7-79-192

August 1979

Calcium Sulfite Crystal Sizing Studies

by

Larry O. Edwards

Radian Corporation
8500 Shoal Creek Boulevard
Austin, Texas 78766

Contract No. 68-02-2608
Task No. 30
Program Element No. EHE624

EPA Project Officer: Robert H. Borgwardt

Industrial Environmental Research Laboratory
Office of Energy, Minerals, and Industry
Research Triangle Park, NC 27711

Prepared for

U.S. ENVIRONMENTAL PROTECTION AGENCY
Office of Research and Development
Washington, DC 20460

CONTENTS

SECTION		Page
1	INTRODUCTION	
	BACKGROUND	1
	PURPOSE	1
		2
2	SUMMARY	
	VISUAL METHODS	3
	INSTRUMENTAL METHODS	3
	NUCLEATION STUDIES	4
		5
3	EXPERIMENTAL METHODS	
	INTRODUCTION	6
	OPTICAL MICROSCOPY	6
	SCANNING ELECTRON MICROSCOPE (SEM)	6
	INSTRUMENTAL COUNTING	15
		16
4	RESULTS OF VISUAL METHODS	
	INTRODUCTORY DISCUSSION OF $CaSO_3$ CRYSTALS	18
	OPTICAL COUNTING	18
	SEM COUNTING	22
		27
5	RESULTS OF INSTRUMENTAL METHODS	
	COULTER COUNTER RESULTS	37
		37
6	NUCLEATION STUDIES	
	INTRODUCTION	52
	GRANULES	52
	PLATELETS	53
		55
7	DISCUSSION OF RESULTS	
	SUMMARY OF VISUAL SIZING METHODOLOGY	58
	COMPARISON OF VISUAL AND INSTRUMENTAL RESULTS	58
	NUCLEATION	59
		61
8	REFERENCES	62
	APPENDIX A - INSTRUMENTAL DATA	63

FIGURES

NUMBER		Page
3-1	Optical photographs of $CaSO_3$ granules in 30% glycerol at 400X magnification.....	8
3-2	Optical photograph of $CaSO_3$ platelet sample that was treated with 60-seconds of ultrasonic dispersion.....	10
3-3	SEM micrograph of $CaSO_3$ platelet sample ultrasonically dispersed during preparation.....	11
3-4	Optical photograph of $CaSO_3$ platlets (not sonicated).....	12
3-5	Optical photographs of granules from a full-scale scrubber, not sonicated.....	14
3-6	SEM photograph of scrubber platelets.....	17
4-1	SEM photograph at 207X of $CaSO_3$ platelets from a full-scale scrubber.....	19
4-2	SEM photograph at 201X of $CaSO_3$ platelets from a full-scale scrubber.....	19
4-3	SEM photograph of laboratory grown granular particles at 300X magnification.....	20
4-4	SEM photographs of laboratory grown granular particles.....	21
4-5	Optical photograph of some laboratory grown $CaSO_3$ platelets; 200X.....	23
4-6	SEM photograph of scrubber-grown $CaSO_3$ platelets, at 2000X...	24
4-7	Graphic display of number count of $CaSO_3$ granular particles..	26
4-8	Optical photograph of $CaSO_3$ platelets.....	28
4-9	Graphic display of the number count of $CaSO_3$ platelet particles.....	29
4-10	Optical photograph of $CaSO_3$ platelets.....	30
4-11	SEM photograph of sonically dispersed sample of $CaSO_3$ platelet; 204X.....	32
4-12	Graphical display of the visual count of SEM photo (200X) of platelets.....	33

FIGURES (continued)

NUMBER		Page
4-13	Graphical display of volume count calculated from number count given in Figure 4-12a	35
5-1	Sieved platelets in size range 8-13 μm	38
5-2	Logarithmic display of number count of platelets in the 8-13 μm size range	39
5-3	Optical micrographs showing results of sieving $CaSO_3$ granules.	41
5-4	Optical micrograph showing results of sieving of $CaSO_3$ platelets from a full-scale scrubber	44
5-5	Optical micrograph showing results of sieving of $CaSO_3$ platelets from an RTP pilot scrubber	47
6-1	Optical micrograph of granules grown from seeded supersaturated $CaSO_3$ solutions	54
6-2	Product platelets from different seeding growth conditions	56
7-1	Graphical display of composite SEM counting (combined sonicated and non-sonicated counts)	60
A-1	Granules in size range 8-13μ; number count	64
A-2	Logarithmic display of number count in Figure A-1	65
A-3	Granules in size range 13-20μ	66
A-4	Logarithmic display of number count in Figure A-3	67
A-5	Granules in size range >20μ; not sonicated	68
A-6	Logarithmic display of number count in Figure A-5	69
A-7	Granules in size range >20μ; sonicated	70
A-8	Logarithmic display of number count in Figure A-7	71
A-9	Platelets in size range 13-20μ; not sonicated	72
A-10	Logarithmic display of number count calculated from volume count in Figure A-9	73

FIGURES (continued)

NUMBER		Page
A-11	Platelets in size range 13-20μ; sonicated.....	74
A-12	Logarithmic display of number count in Figure A-11.....	75
A-13	Platelets in size range 8-13μ.....	76
A-14	Logarithmic display of number count in Figure A-13.....	77
A-15	Platelets in size range 5-8μ.....	78
A-16	Logarithmic display of number count in Figure A-15.....	79
A-17	Platelets in size range >20μ.....	80
A-18	Logarithmic display of number count in Figure A-17.....	81
A-19	Platelets in size range 13-20μ; not sonicated.....	82
A-20	Logarithmic display of number count in Figure A-19.....	83
A-21	Platelets in size range 13-20μ; sonicated.....	84
A-22	Logarithmic display of number count in Figure A-21.....	85
A-23	Platelets in size range 8-13μ.....	86
A-24	Logarithmic display of number count in Figure A-23.....	87

TABLES

NUMBER		Page
4-1	DETERMINATION OF FINE PARTICLES MISSED AT 200X MAGNIFICATION; OPTICAL MICROSCOPE	27
4-2	DETERMINATION OF FINE PARTICLES "MISSED" AT 200X MAGNIFICATION; SEM	31
5-1	ESTIMATES OF CENTRAL TENDANCY FOR VOLUME COUNT ON GRANULES OF $CaSO_3$ BY THE COULTER METHOD	42
5-2	LOG-NUMBER SLOPES OF SIEVED GRANULES	42
5-3	ESTIMATES FOR CENTRAL TENDANCY FOR VOLUME COUNT ON $CaSO_3$ PLATELETS BY THE COULTER METHOD FOR FULL SCALE SCRUBBER	45
5-4	ESTIMATES FOR CENTRAL TENDANCY FOR VOLUME COUNT ON $CaSO_3$ PLATELETS BY THE COULTER METHOD FOR PILOT SCALE SCRUBBER	46
5-5	LOG-NUMBER SLOPES OF SIEVED PLATELETS FROM FULL-SIZE SCRUBBER	49
5-6	LOG-NUMBER SLOPES OF SIEVED PLATELETS FROM RTP PILOT SCRUBBER.	50

SECTION 1

INTRODUCTION

1.1 BACKGROUND

Sludge disposal represents a significant operating cost in most applications of lime/limestone or dual alkali scrubbing processes. In systems where calcium sulfite is the major product, the waste sludge generally settles slowly, has a low settled density and is difficult to dewater. An earlier EPA report [1] developed a mathematical model of a scrubber to improve the quality of calcium sulfite sludge. It was assumed that the size distribution of calcium sulfite crystals can be used to predict sludge quality for most systems. That report related the crystal size distribution to process conditions. By using a mass-balance approach in which the change in the number of crystals in a size range is equal to the net flux via convection and via growth, a mathematical statement of the problem was derived:

$$\frac{d(Rn)}{dL} - n\sum_j \frac{1}{\gamma_j} + D(L) = \sum_i \frac{n_i}{\gamma_i} + B(L) \qquad (1\text{-}1)$$

where: L = one dimensional crystal characteristic dimension

γ_i = inlet time constant = $\frac{\text{vessel volume}}{\text{stream flow rate}}$

γ_j = outlet time constant = $\frac{\text{vessel volume}}{\text{stream flow rate}}$

$R(L)$ = crystal growth rate

$B(L)$ = crystal birth function by other than nucleation

$D(L)$ = crystal death function

$n(L)$ = crystal size distribution function such that $n(L)\Delta L$ is the number of crystals in the size range (L) to $(L + \Delta L)$ per unit volume of slurry.

This equation is essentially a conservation equation which simply accounts for all sources and sinks and flows of crystals. The reader is referred to the previous EPA report [1] for further details of derivation and application.

The model depends upon nucleation and growth rate parameters. These quantities are determined from experimental measurement of the crystal size distribution n(L). The linear growth rate R(L) is determined from the slope of the crystal size distribution curve and the solids residence time. Since the nucleation birth rate B_o, which enters the differential (Equation 1-1) as a boundary conditions, is defined as the limit of the population times the growth rate for very small particles.

$$B_o = \lim_{L \to o} n(L)R(L), \qquad (1\text{-}2)$$

the nature of n(L) in the small particle range is very important. The success of this type approach depends upon the function chosen to approximate n(L). In the earlier work [1], n(L) was measured by several means for two full-scale scrubbers. However, the variety of methods led to two rather contrary results for n(L): (1) instrumental results gave a particle number count exponentially increasing with decreasing particle size; (2) optical microscope and sieving gave a number count which increased to a maximum but then decreased toward zero for smaller particles. That report recommended clarification of this discrepancy.

1.2 PURPOSE

The purpose of the current work was to resolve the discrepancy in the measured values of n(L), if possible, to provide an analytical function for n(L), and to recommend the best method for the routine sizing of particles. In particular, a reliable method was sought which would at least approximately measure the slope in the small particle region (<2 μm) for n(L) versus L. An understanding of the physical factors influencing the nucleation process is valuable when trying to produce a higher quality sludge. Thus, as time and resources permitted, laboratory, batch nucleation studies were to be used to quantify some of the factors influencing calcium sulfite nucleation. Specifically, the effects of temperature, concentration, pH, energy input (stirring) and seeding were considered.

Two types of crystal forms are known to exist in full-scale scrubbers. One shape is a flat platelet, previously judged to be about 1:20:30 in relative thickness:width:length. The other shape is granular and sphere-like, although not always regular. The platelets are more dense and settle faster and are the preferred morphology. The physical relation between the two forms, if one exists, was not discerned in the previous study. It was hoped that the nucleation studies could identify factors which influence the crystal's form.

SECTION 2

SUMMARY

2.1 VISUAL METHODS

The scanning electron microscope shows that $CaSO_3$ platelet crystals are not flat, but tend to thicken in the middle. Visual methods, by both light and electron microscopes, with manual counting do not produce a reliable particle size distribution for $CaSO_3$ crystals because they cannot measure the thickness of the crystals. For the same reason, sieving, which segregates platelets by area, also cannot produce a reliable particle size distribution.

Visual methods can be used for a quick survey of the crystals. The general size and geometry of the particles are readily apparent, as is the presence of any significant amount of impurity or other particle type. A series of samples from the same source may have a fairly consistent thickness-to-width ratio, and visual inspection may be useful in qualitatively determining relative sizes.

Visual sizing of $CaSO_3$ granules suffers from three drawbacks: they are nearly transparent at their edges, they frequently clump together, and there are numerous voids which make true particle volume uncertain.

It was discovered in the course of this work that the granules are actually hundreds of small platelets growing out of a common center. These particles are nearly spherical and contain many internal void spaces. This explains why they are less dense, settle more slowly and dewater more poorly than the individual platelets. SEM work clearly showed the platelet-like fine structure of the granules. Many intermediate particles also showed multiple platelet growth from one platelet, but not enough platelets to form a sphere. Nucleation studies, summarized in Section 2.3, showed that the granules form when rapid growth occurs; individual platelets grow slowly and only in slightly supersaturated solutions of $CaSO_3$. Hence, even the definition of a "single" particle (granule), which is composed of many small platelets, may be uncertain.

In the particle sizing and counting work, a granule was considered to be a single particle in granular sediments, and an individual plate was considered as a single particle in platelet sludges.

2.2 INSTRUMENTAL METHODS

Instrumental counting is commonly done by either of two techniques, Coulter Counter or sedimentation. The manufacturers' literature and the results of work done in the report cited above indicate that the two techniques are nearly equivalent. In this work, we report results only for the Coulter method.

The Coulter method measures the particle's volume and reports it in terms of an equivalent spherical diameter (ESD). When several platelet samples from different sources were sieved into the same size range (by area), very different ESD's were reported. This indicated that thickness-to-width ratios of crystals from different sources vary appreciably. However, for a series of $CaSO_3$ platelets grown in the same source, Coulter results paralleled expectations based on sieving. The Coulter method is fast, yields repeatable results, is well suited for determining the ESD's and is excellent for comparing size distributions.

If the number-size data are plotted on a logarithmic scale, they are represented fairly well by several straight lines. This means that the population is multimodel and each mode is exponential. However, most crystal population theories predict one line (slope) for a particular sample; two or three were nearly always found in this work. Speculation on crystal growth mechanics that would produce such a multi-model population was addressed in the EPA report cited above [1]. The exponential dependence of particle number on size is in the form most compatible with the mathematical model. Future use of that model will likely involve the determination, by instrumental methods, of a multi-termed, exponential, number-size function.

The very large numbers of small particles as reported by the instrumental counting techniques in the earlier work implying high nucleation rates were almost certainly fly ash particles. The sludges used were from on-line, full-scale scrubbers. Work reported in this paper on pilot scrubbers (without fly ash) indicates that extrapolation of the particle size distribution curve to zero size to estimate the birth rate (Equation 1-2) is valid for fly ash-free systems.

Preparation of the sample by using ultrasonic dispersion is not recommended. While it may break up some agglomerations, invariably they quickly (re)form. And sonication does erode the edges and corners of the platelets. In all cases but one, the size of the particle was reduced after sonication. While some of the differences were significant on a volume-count basis, there was less effect in the number-count presentation.

Number-size trends for the granules appeared to be more regular than those for platelets. Size comparisons between samples from the same source, as determined by the Counter method, should be quite reliable. Since the granules are really formed from platelets, sonication also erodes these particles and is not recommended prior to instrumental counting.

2.3 NUCLEATION STUDIES

$CaSO_3$ nucleation mechanisms were also studied. The ultimate goal was to understand processes which control the formation of calcium sulfite sludge. In batch experiments, crystals were grown in a variety of environments that simulated scrubber conditions. The effects of pH, impeller speed, concentration, temperature, kinetics and seeding on both crystal morphology (platelets or granules) and size were monitored.

The following conclusions were reached:

- Solution temperature and stirring speed have little effect upon crystal type or size.
- $CaSO_3$ crystals do not form at a pH of below 3.2, where bisulfite is the dominant ionic form.
- In very supersaturated solutions (greater than three times saturation), granules invariably form.
- Whenever spontaneous nucleation occurs the resultant crystalline form will be granular.
- Platelet $CaSO_3$ crystals can only be grown (in batches) at low supersaturation levels with platelet seeding.
- The resultant size (area) of crystals grown by using seeds appears independent of the size of the seed crystals. This may not hold for the volume size.
- Granules dissolve more readily than do platelets in mild acid, probably because the granules have a much larger relative surface area. Hence, SO_2 scrubber contactors may be preferentially destroying the granular forms.

SECTION 3

EXPERIMENTAL METHODS

3.1 INTRODUCTION

Many particle sizing methods exist; a survey of the prominent techniques was made in a previous Radian-EPA report [1, Appendix C]. In this report the more applicable methods have been explored in greater depth and compared to the others:

- optical microscopy,
- scanning electron microscopy (SEM), and
- Coulter counting.

The Coulter method is instrumental and is preferred for frequent use because of its ease of use, the large size of the sample counted, and its unbiased (by operator) results. Manual counting, whether on optical micrographs or scanning electron micrographs, is very susceptible to error. Inaccuracies arise because the number of particles counted is small and discretion must be used by the observer; the counting is also very time consuming. Consumption of time is not in itself a cause of inaccuracy. Instrumental methods survey much larger, hence statistically better, samples. Each of these techniques will be discussed and compared to the others in detail below.

3.2 OPTICAL MICROSCOPY

A conventional optical microscope is certainly the simplest method available for quickly surveying a sample of crystals. The general shapes, the approximate size, and any major contaminants can be seen, but quantification of these observations is difficult.

3.2.1 Mounting Techniques

Mounting crystals for microscope viewing is very important. A brief description of several techniques is given in this section along with the advantage and disadvantage of each.

Placing a drop of slurried $CaSO_3$ crystals on a slide leads to a variety of problems. The larger crystals are found near the center of the drop;

the smaller ones seem to be prominently near the edges. $CaSO_4$, always present to some extent in these $CaSO_3$ solutions due to oxidation, forms crystals at the edge of the droplet. If the drop is allowed to dry, clusters of crystals form and $CaSO_4$ appears throughout.

The microscope's depth of field is shallow and all of the crystals in the drop cannot be simultaneously in focus. If a cover slip is placed on top of the droplet, the depth of field is improved, but pressing the cover slip down enough to get a thin layer of crystals causes crystal breakage. Also, differential migration (by size) is observed as the smaller crystals move to the edge of the coverslip; see Figure 3-1.

Dried sludge dusted onto a slide gives good contrast, but crystals may break under the coverslip and there is much agglomeration. There is no assurance that dusting maintains the original size distribution.

Immersion of the $CaSO_3$ crystals in oil or grease will protect the crystals from breakage and help disperse agglomerates. The oils tested in this study included glycerol, silicon oil, nujol, fluorolube and silicon vacuum grease. The refractive index of the oil used must be substantially different from the refraction index of the crystals to prevent loss of contrast.

Most oil-crystal mixtures showed aging changes: Some reaction, probably dissolution, occurred slowly, and samples viewed several hours after immersion were obviously altered. In the less viscous oils, differential migration was apparent; certain areas of view would consist predominantly of large crystals while others contained only small crystals; again see Figure 3-1. The greases did not disperse agglomerates very well.

Filtering slurried crystals onto a Millipore® filter was often adequate for good viewing, but agglomerates frequently formed and smaller particles could have been lost through the filter or obscured by larger particles. The best preparative technique developed for $CaSO_3$ crystals was aspiration of slurried crystals onto a Millipore filter (with no suction); the filter was at no time saturated with water, and drying was allowed between aspirations. This technique appeared to hold crystals where they impacted, and agglomerations were fewer. Breakage was expected to some degree, but little evidence (i.e., irregular breakage angles plus oddly shaped bits and pieces) was observed. Also, the amount of $CaSO_3$ deposited from the drying of the saturated $CaSO_3$ solution was calculated to be a very small fraction of the total crystal weight.

After the crystals were distributed onto the dried Millipore filter substrate, pieces were cut from the filter body, placed on a slide and immersed breifly in acetone vapor. The acetone vapor changes the Millipore substrate into a clear plastic film suitable for optical transmission microscopy. The process is rapid (a few seconds), and no change in the $CaSO_3$ particles is apparent.

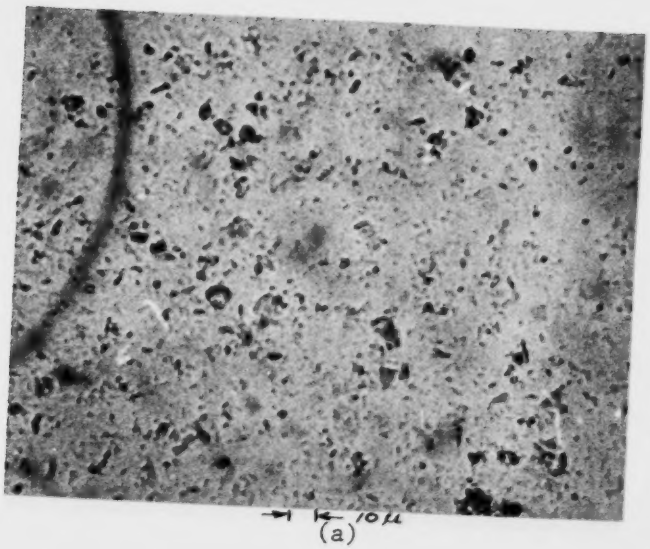

(a)

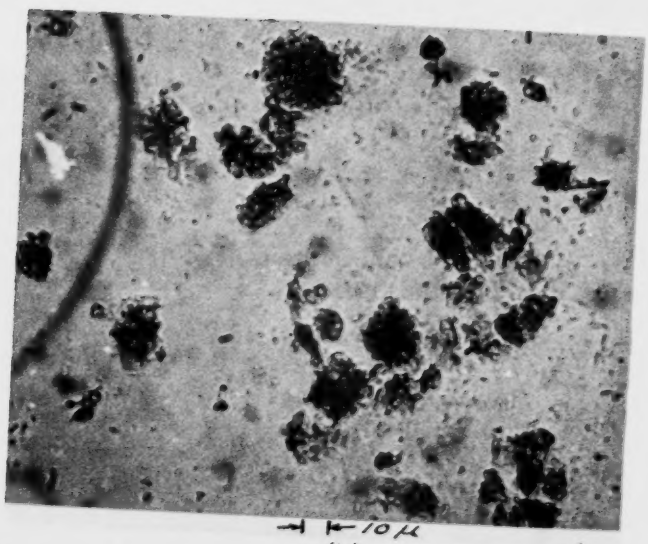

(b)

Figure 3-1. Optical photographs of $CaSO_3$ granules in 30% glycerol at 400X magnification. The two micrographs (a) and (b) were taken on the same slide only a few millimeters apart.

A special mention should be made of sonic dispersion. Recommended procedure for use of a Coulter Counter includes immersion for 60 seconds in a commercial ultrasonic vibrator bath. In anticipation of comparisons, the effects of sonication were also investigated by microscopy. This treatment of a few milliliters of crystal slurry does break-up agglomerates, but it also appears to erode the crystals, as evidenced by the broken edges of platelets shown in Figures 3-2 and 3-3. While only a few, new smaller broken shards are observable, the larger platelet crystals look as though they have been chipped away. The edges of the granules are too indistinct to be resolved, but no change upon sonication is discernible. Finally, it should be noted that the crystals rapidly reagglomerate (although probably not as strongly); they definitely have an affinity for one another. A further discussion on the effects of sonication is given in the section on instrumental counting; see Section 5.

3.2.2 Microscope Techniques

Although the use of a conventional microscope is relatively straightforward, several techniques were tried to increase contrast and distinguishability. However, none resulted in any significant improvement.

Various stains and dyes were tried. While they were picked up by the crystals and color vision was improved, black and white contrast on Polaroid photos was not improved. Immersion oils were also tried, and while they enhanced clarity at high magnifications (1000X and 2000X), nothing additional was seen at these magnifications. Also, the oils tended to dissolve some of the crystals, especially the fines. Off-center lighting slightly improved boundary definition. Polarization methods, useful for single crystal work, were of no particular advantage in counting or sizing fields of crystals.

Multiple photographs were taken of the same area at different magnifications. As the magnification was steadily increased, it was found that few free particles were being missed in the less magnified photographs. If smaller particles are there, this technique is not able to detect them. However, many smaller $CaSO_3$ platelets were revealed clinging to or growing out of the larger platelets. Light polarization microscopy also confirmed the presence of smaller crystals on the surfaces of large ones. These adhering platelets were normally not counted as separate particles. Their exact number and size were usually unresolvable, see Figure 3-4.

The $CaSO_3$ granules clustered together and showed such a complex inner structure that increased magnification revealed no new useable information, see Figure 3-1. Within the range of conventional optical microscopes, magnification greater than 200X proved to be of little additional use in counting or sizing $CaSO_3$ particles.

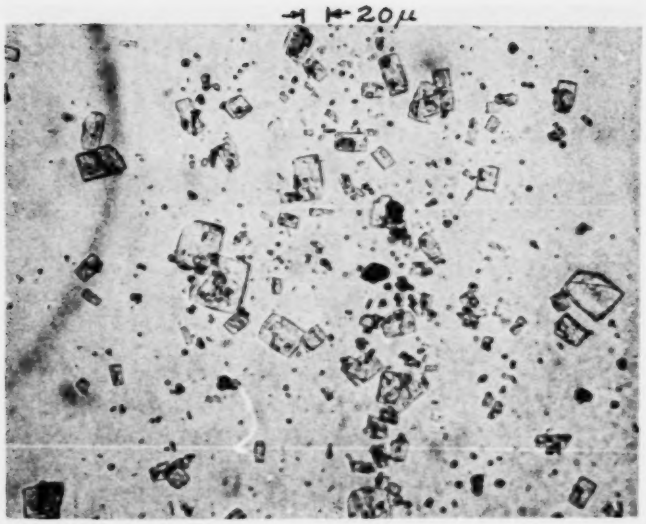

Figure 3-2. Optical photograph of $CaSO_3$ platelet sample that was treated with 60-seconds of ultrasonic dispersion. Note the many broken or eroded corners and edges as well as some broken, non-rectangular smaller particles; 200 X magnification.

Figure 3-3. SEM micrograph of $CaSO_3$ platelet sample ultrasonically dispersed during preparation. Magnification at 501X. Note irregularities around edges and on corners. Also note notches in the ends of many crystals.

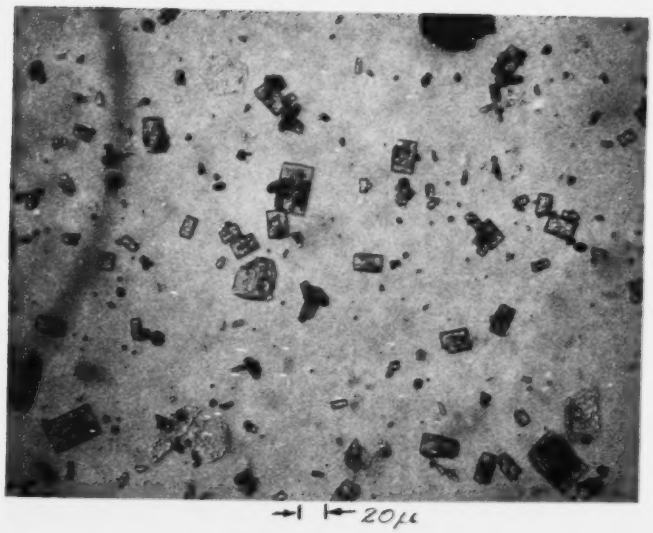

(a)

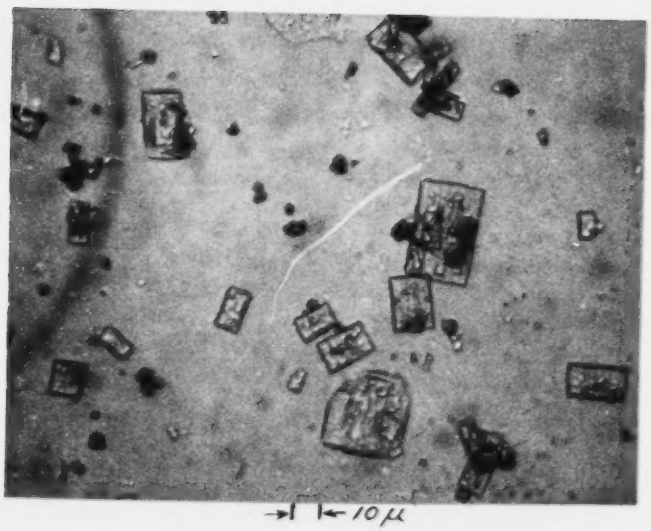

(b)

Figure 3-4. Optical photograph of $CaSO_3$ platelets (not sonicated).
a) typical field at 200 magnification
b) same area (near center) as above at 400 magnification.
Note that essentially no "new" particles are resolvable at 400X that were not identifiable at 200X. The multiple crystal nature of a "single" platelet is more clearly revealed.

3.2.3 Counting

Counting is very discretionary. First, one must decide which field to select for counting. Then one must determine how many particles to count. Additionally, it must be decided exactly what a particle is. For the reader more interested in this phase of the work, each of these points is addressed below.

For almost any preparative technique, areas with varying particle density will be seen in the microscope field. Some uncountable agglomerations will be present. The more sparsely populated areas are easier to count, but the number of particles counted is small, and one must decide if the exclusion of agglomerations can be justified. Also, some areas will have a greater abundance of large (or small) particles, due either to normal statistical fluctuations or size differential migration of particles during preparation, see Figure 3-1. The observer must decide what a truly representative area is.

Secondly, one must decide how many particles constitute a "good" statistical sample. Certainly, the larger the count the better the sampling, but one usually is limited by time and resources. The count totals by instrumental methods can be quite large, and one cannot hope to visually count a comparable number of particles. Optically, perhaps the best one can do is to terminate the count when it is observed that the distribution is not "significantly" changing.

Thirdly, for platelets, it must be recognized that one cannot be sure of the crystal thickness. The $CaSO_3$ platelets are too thin to measure on an optical microscope. Realistically, to get a volume count, some ratio of thickness-to-width must be assumed. While this may produce fairly constant results for each sample, the thickness ratio may vary according to the sample history. Comparison with instrumental counting (see Section 5) indicates that the thickness-to-width ratio may vary significantly for different samples of $CaSO_3$ platelets.

The granules presented other similar problems and were difficult or impossible to count. Several attempts were made, but results were not conclusive. For example, refer to Figure 3-5. Figure 3-5a is a photograph at 400X magnification of a batch of $CaSO_3$ granules aspirated onto a substrate without sonic dispersion. Counting the distinguishable dark spots as separate particles still raises many questions. Some spots are rather more faint than others; should they be counted equally? Are overlapping spots separate particles? How large are particles partially obscured by other bodies? Figure 3-5b is an enlargement of an area of Figure 3-5a. While some detail is resolved, none of these discretionary questions is clarified. Circular templates were used to estimate the area of each circular dark spot in the photograph.

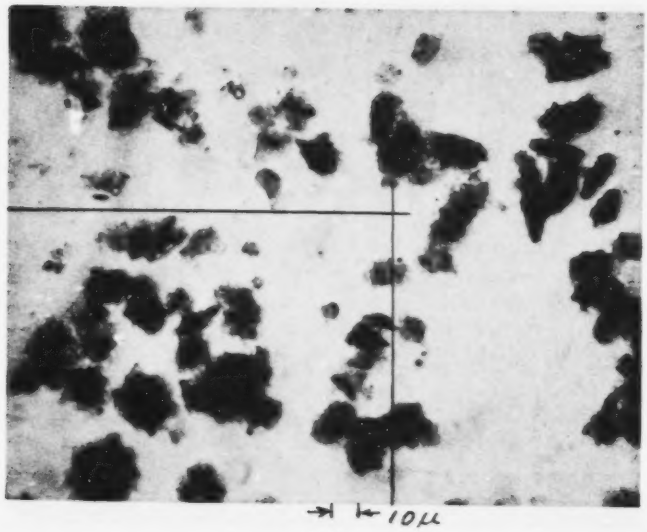

(a)

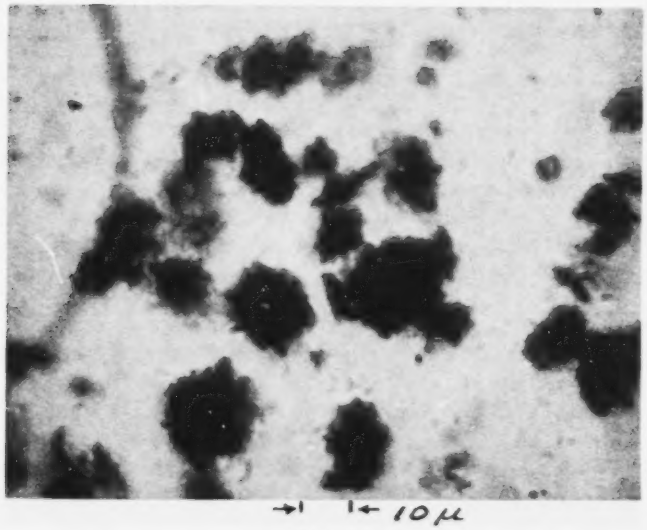

(b)

Figure 3-5. Optical photographs of granules from a full-scale scrubber, not sonicated;
a) 400X
b) 800X of area in box in (a)
Note irregular shapes and difficulty in defining individual particles. Also a vast number of small particles is not apparent. A count of (a) is shown in Figure 2-12.

Finally, for platelets, one must decide what to call a particle. This can be most difficult, and those definitions may vary with one's objective. For example, is an agglomerate to be counted as a single particle? Should a single platelets with several smaller ones adhering to its surface be counted as one or several particles? Should bits of foreign matter (like fly ash or limestone) be counted? Should particles growing out of other particles be counted separately? The granules present other similar problems, and they are more difficult or impossible to count.

When sizing particles for comparison with instrumental methods (which don't distinguish between crystal types), all free particles, with agglomerates counting as one, should be counted. When determining the number of nucleation events, all independent $CaSO_3$ particles should be counted. When counting to predict sedimentation rate, particles with different dry densities or shape factors should be counted separately.

In addition, one must decide whether a visual irregularity on a crystal is a separte crystal, a new nucleation site, or just a structural irregularity. Individual particles within an agglomeration can only be counted approximately, if at all.

All these factors are at the discretion of the counter. The process is tedious, time-consuming and could produce a wide spectrum of measurements for the same sample. Thus, while it is a good method for a quick survey, and it can distinguish between different types of particles, optical micrography can be a most difficult and potentially imprecise crystal sizing method.

As explained in the preceding sections, optical counting has its benefits and drawbacks. Some of the difficulties are overcome if the purpose of the count is well defined. A discussion of the results will be postponed until after the section on the SEM work, at which point the two visual counting methods will be compared.

3.3 SCANNING ELECTRON MICROSCOPE (SEM)

The SEM was used to look at the crystals in more detail and to look into the size range below 5μ where the optical microscope becomes unreliable.

The mounting technique that appeared to work best for optical microscopy was also used for SEM. That is, a fairly dilute slurry of $CaSO_3$ crystals was aspirated onto a fine Millipore filter and allowed to dry. This method yielded the most uniform distribution and minimized agglomerations and breakage. The samples were then optically inspected, photographed and counted. Subsequently, a small piece of filter, about 2 mm on a side, was cut out and mounted on an SEM stage. It was sputtered with gold and carbon to provide the conducting medium necessary for the SEM.

Counting particles in an SEM micrograph is somewhat easier than in an optical micrograph because of improved resolution and depth of field. However, discretionary problems are heighthened. Multiple crystal formations are more distinguishable, and a refined definition of particles is necessitated; see Figure 3-6. In Figure 3-6b, how many particles are seen? Other difficulties discussed in the counting of optical micrographs apply equally to counting of SEM micrographs; see Section 3.2.3. Points made in Section 3.2.4 are also applicable to SEM work.

3.4 INSTRUMENTAL COUNTING

In this work, two types of instrumental size counting techniques were considered, Coulter Counter and sedimentation. Commercial sedigraphs (e.g., Micromeritics Instrument Corporation) require several grams of materials and the sieving procedures described below yielded only milligram quantities. Thus, only Coulter Counter data will be reported. In other similar work ([1], Appendices C and D), including Micromeritics' own literature, the sedimentation results are nearly identical to other instrumental results (Coulter Counter).

The Coulter Counter (Coulter Electronics, Inc.) instrument employs an electrical current flowing across a small aperture in a conducting solution. As the solution flows, particles passing the aperture raise the electrical resistivity approximately in proportion to their size. A signal constitutes a count, and a measure of the volume of conducting solution displaced is related to the volume of the particle. If the solution is too concentrated with particles, coincidence counts will result in several smaller particles counting as one larger particle. Coulter results, if in error, will favor the larger particles. The ease of operation and reproducibility of results make this method very desirable if many routine analyses are needed.

The samples, both granules and platelets, were analyzed at the Coulter Electronics Lab. They were analyzed in a 4% $NaCl/H_2O$ solution saturated with $CaSO_3$ and filtered. A Coulter Counter Model TAII with 140 μm and 50 μm apertures was used. When sonicated, the samples were placed in an ultrasonic bath for 60 seconds. The data were processed on a Coulter M3 data processor/calculator system. In most cases the particle size distribution (PSD) was recorded as the number and volume percents finer than each size range.

In certain experiments described later, crystals sieved into size ranges were counted (Section 5) and used for seeding (Section 6). Micromesh sieves were used with the aqueous $CaSO_3$ slurry. A repeated pull-push vacuum was used to thoroughly wash the crystals. With this method about 500 mg could be sieved at a time with about 2 liters of saturated $CaSO_3$ for washing. The various size fractions were then stored in saturated $CaSO_3$ slurries.

(a)

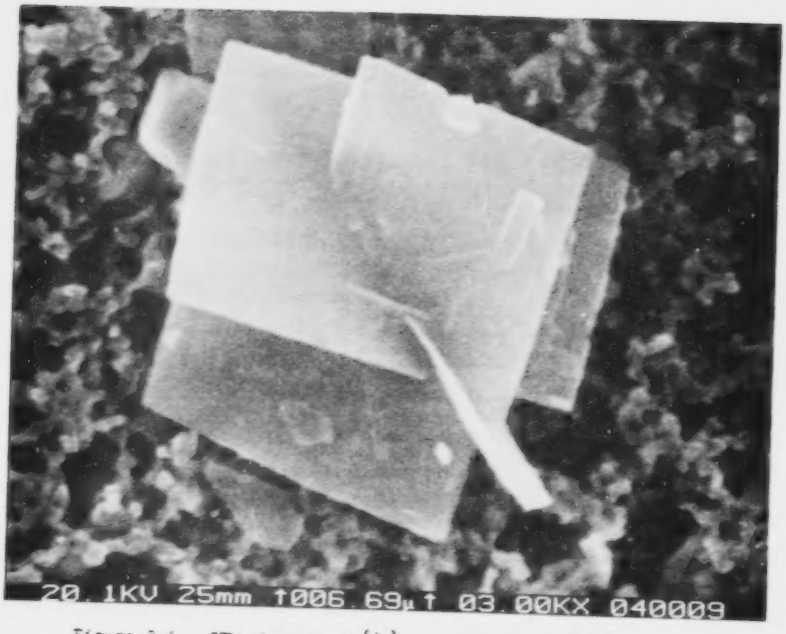

Figure 3-6. SEM photograph (of) scrubber platelets.
a) 500X
b) 3000X of area in (a) at lower left tilted by 40°.
Note in (a) multiple incidents of crystals growing out of crystals. (b) is a particularly graphic example of this. Also note the small thickness of platelets.

SECTION 4

RESULTS OF VISUAL METHODS

4.1 INTRODUCTORY DISCUSSION OF $CaSO_3$ CRYSTALS

Inspection of the SEM photos reveals several useful and interesting facts about the $CaSO_3$ samples used. Since the platelet samples were from a full-scale working scrubber, some limestone was observed; see Figure 4-1. The limestone was usually in an ovoid shape with no angularities. There was not enough limestone present to affect the total particle count. The particles that were seen were fairly large (>3μ), and an elemental analysis (by electron induced emission on the SEM) showed almost pure calcium. It should be noted that only elements heavier than sodium are amenable to SEM analysis.

Fly ash, previously unnoticed by optical microscopy, was detected by SEM. In fact, large numbers of small particles were observed. Almost all the fly ash was smaller than 2μ and spherical; it was easily distinguishable from the $CaSO_3$ crystals. An elemental (heavier than sodium) analysis of the fly ash yielded a rather typical distribution. In order of approximate abundance: Si, Al, Fe, P, Ca, Cl, Ti, K.

The morphological details are also more clearly seen with the SEM. As observed elsewhere, crystal growth out of the face of parent crystals is a very common crystal nucleation and growth mechanism. The enlargement frame, or cursor, in Figure 4-2 shows in detail a complex network of crystals growing out of the surface of a 20 x 30μ crystal. Inspection of this and other photos confirms the fact that secondary growth is very common. Figure 3-6b is even more dramatic; it is a close-up, tilted somewhat, of the crystal complex in the lower left corner of Figure 3-6a.

The $CaSO_3$ granules are actually multiple growth centers on one parent platelet. Figure 4-3 clearly shows platelets with "spine-like" projections covering them. Here, the parent platelets are still resolvable, whereas in Figure 4-4a, the parent rectangular shape has nearly been obscured. An enlargement of the large granule very near the center of Figure 4-4a is shown in Figure 4-4b. Clearly, the "spines" are rectangular platelets in great numbers growing radially out of a center that had provided sites for multiple secondary nucleation. This photo is also typical in that many of the platelets grown in the same solution seem to be nearly the same size.

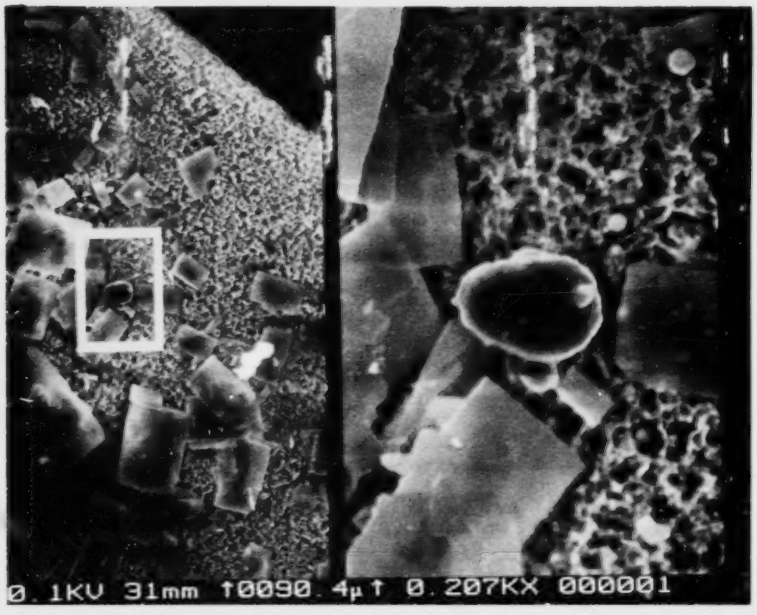

Figure 4-1. SEM photograph at 207X of $CaSO_3$ platelets from a full-scale scrubber. Cursor at the right is 5X the 207X magnification. Note fly ash (small, white spheres) scattered about; its elemental analysis in decreasing order is: Si, Al, Fe, P, Ca, Cl, Ti, K (only elements heavier than sodium are detected). The ovoid shaped particle in the cursor is limestone. Background is a millipore filter.

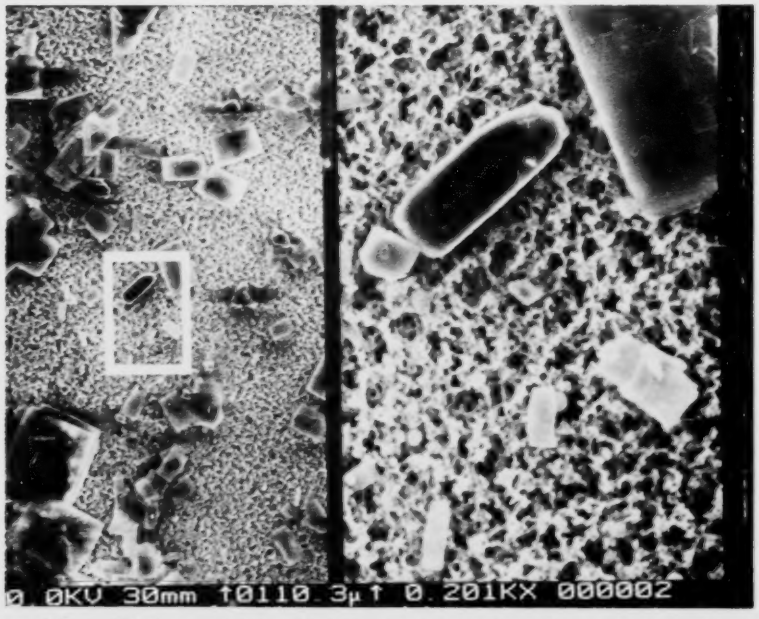

Figure 4-2. SEM photograph at 201X of $CaSO_3$ platelets from a full-scale scrubber. Cursor at right is 5X the 201X magnification. Dark, ovoid particles are limestone. Note details of secondary crystal formations on larger platelets.

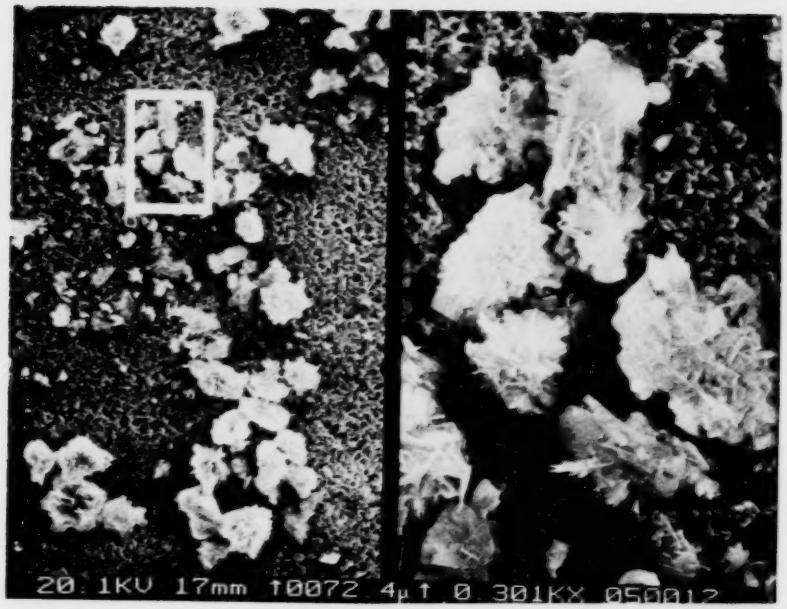

Figure 4-3. SEM photograph of laboratory grown granular particles at 300X magnification. Cursor area at right is 5X the 300X magnification. Multiple plates seem to be growing out of parent platelet eventually to form nearly spherical body.

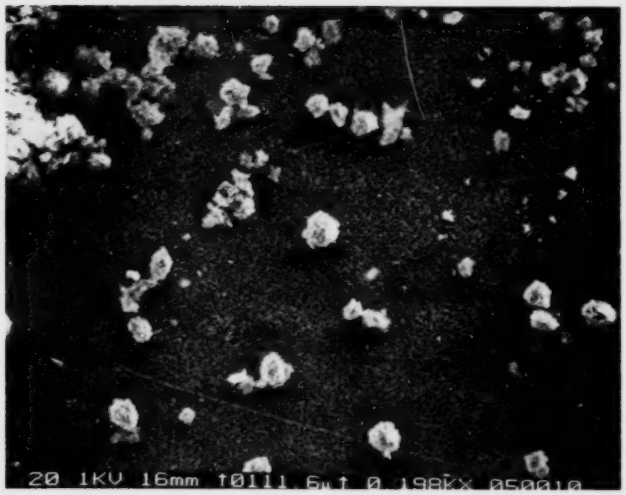

(a)

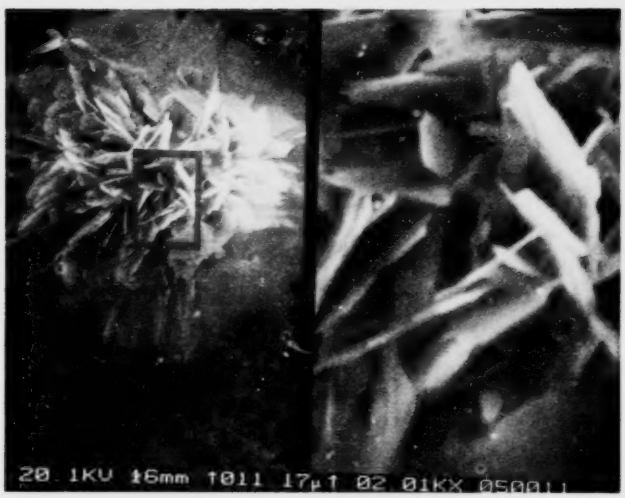

(b)

Figure 4-4. SEM photographs of laboratory grown granular particles.
a) 198X
b) 2000X (cursor at right 10,000X); this particle is the large granule near the center of (a).
Note carnation appearance of dense maze of plates. Also, note extreme thinness of plates; at the bottom of (b), on the left, the plates are so thin as to be transparent. In (b) on the right, the thickness is no more than one-sixtieth of the width.

Many distributions were observed in the course of this work. Nearly always there seemed to be an abundance of crystals at a certain size, and almost none larger. Figure 4-5 represents a batch of laboratory grown platelets where one size seems predominant. Apparently, once the crystals reach a certain size under these individual growth conditions, some other type of growth dominates. It appears that many of these "large" crystals began as secondary nucleations, and once a certain size was reached, they broke off. Note the many crystals with notches in one end, where the crystal was apparently nucleated and later broken off. Again, refer to Figure 3-6b; it is believed that this is a crystal complex before these "mature" crystals break off.

Figure 4-4b also provides a good opportunity to measure the thickness of a platelet. It is impossible to determine whether any one platelet is being viewed exactly edge on. But in the "carnation-like" granule, where the length and width are fairly consistent, the thinnest edge-on view measures about one-fiftieth to one-sixtieth of the width. One cannot be sure any view is exactly edge-on, and some further rotation may reveal the crystal edge to be even thinner. This ratio would then represent a maximum possible thickness assuming that the length-to-width-to-thickness ratios are approximately constant for this platelet morphology.

Other results indicate that some particles may vary considerably in thickness (i.e., thickness-to-width ratio). SEM photos taken of platelets on edge show a wide variability, see Figure 4-6. Breakage may produce particles excessively thick in relation to their length and width; the large particle in the center of Figure 4-6 appears to be broken in this manner. At the same time, the other end of this same platelet appears to be much thinner. Also, the particle immediately beneath it has an air-foil shaped cross-section and appears to be very thin toward its edges. In fact, the thickness-to-width ratio for crystals in this micrograph alone varied from 1:20 to 1:60. Necessarily, the thickness measurement was very imprecise.

Thus, the assumption of a fairly regular thickness-to-width ratio may not be a good one. Even in the same sample, a factor of 3 in the thickness-to-width ratio exists. For different samples, the history of the sample could markedly affect the thickness of the plates. Instrumental results (Section 5) also seem to indicate an inconsistent thickness-to-width ratio.

4.2 OPTICAL COUNTING

The difficulties inherent in visual counting have already been discussed. Discretion must be used by even an impartial observer and the results are necessarily biased, but usually in an unknown direction.

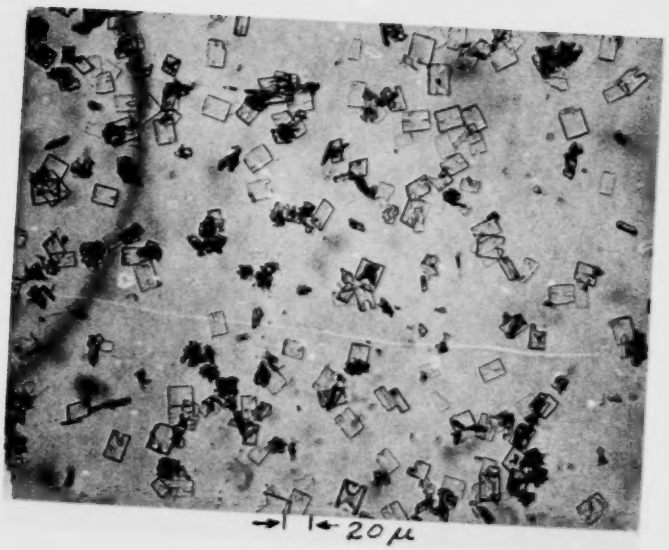

Figure 4-5. Optical photograph of some laboratory grown $CaSO_3$ platelets; 200X. Note predominance of crystals of about the same size. Also note many crystals with notches in the end indicating that the platelet was broken off from growth (nucleation) center

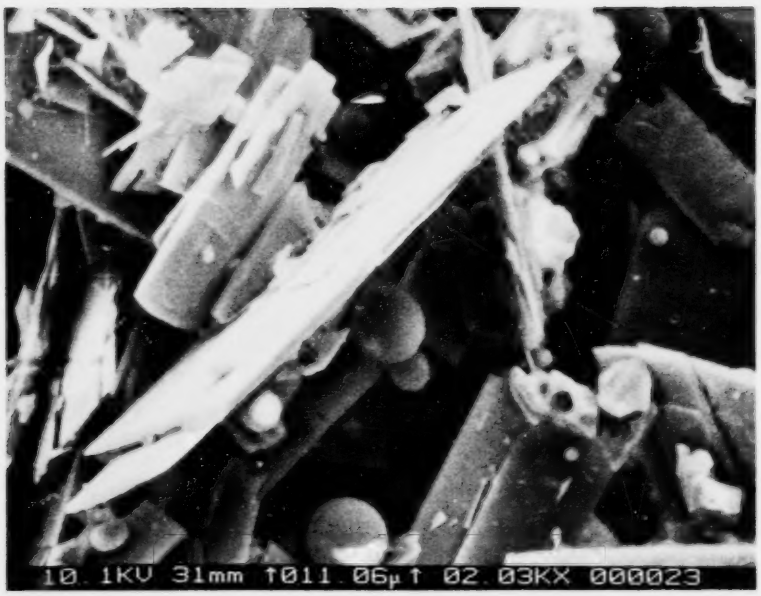

Figure 4-6. SEM photograph of scrubber-grown $CaSO_3$ platelets, at 2000X. An edge view of crystals. Note great variability in thickness between crystals or even for same crystals. The large crystals in the center appear to be thicker toward their center; the largest crystal is believed to be broken at its left end.

4.2.1 Granules

As mentioned in Section 3.2.3, the granules were very difficult to count. Poorly resolvable boundaries and agglomerations were the most troublesome problems. Circular templates were used to estimate the area of each approximately circular dark spot on the photographs; see Figure 3-5. A count of this figure is displayed in Figure 4-7a.

Figure 4-7b represents a count of a similar photograph (actually the photograph in Figure 3-1a) for the same initial sample but after sonic dispersion. (Note: there is a difference in mounting technique between the two figures, but it is not judged to be important in this comparison.) However, the uncountable background appeared much more cluttered in the sonicated sample. Compare Figure 3-5a at 400X to Figure 3-1a at 400X. In the former, the background looks "clean", and no small particles are apparent in the enlargement (Figure 3-5b). But Figure 3-1a shows a myriad of small, unclear spots. Such increases in background "noise" upon sonication were not always this dramatic, but a general trend toward more, smaller particles in sonicated samples was noticed. Finally, to once again emphasize the discretionary nature of the technique, Figure 3-1b pictures an area less than 2mm away from the area shown in Figure 3-1a on the same slide. Because even matched samples often showed considerable variation in appearances, all microscopic and SEM results must be considered to be only qualitative.

4.2.2 Platelets

Particle definition was easier with the $CaSO_3$ platelets than with the granules. Frequent clumps (agglomerates) were uncountable, but these were assumed to be random conglomerations of all types of particles with an approximate average distribution. Thus, to be tractable, the areas chosen to be counted simply avoided such clumps of platelets.

Confusion can arise in the definition of platelet size. Instrumental counts measure a particle's volume and report sizes as equivalent spherical diameter (ESD). Visually one sees flat rectangles with an average ratio of 2:3 for width:length. One can therefore describe the "area" of the particle on the basis of one linear dimension; i.e., width, length or the average of the two. To convert from area to ESD for platelets (to facilitate later comparison):

$$4/3\pi R^3 = t \times w \times \ell \qquad (4\text{-}1)$$

where t is the thickness and 2R = ESD. The typical crystal morphology determined in this work on the SEM indicated an average geometry of 1:30:45, resulting in the crystal width being 2.18 times the ESD. Since the platelet shape factor can vary considerably, this ratio should be used only as an approximate conversion factor.

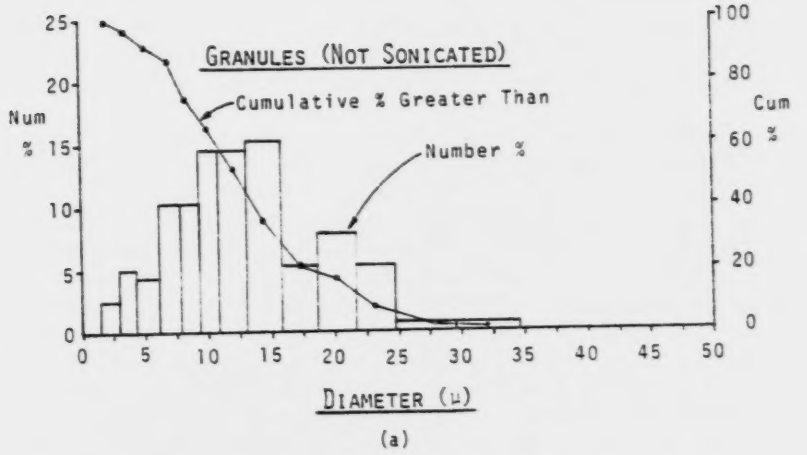

(a)

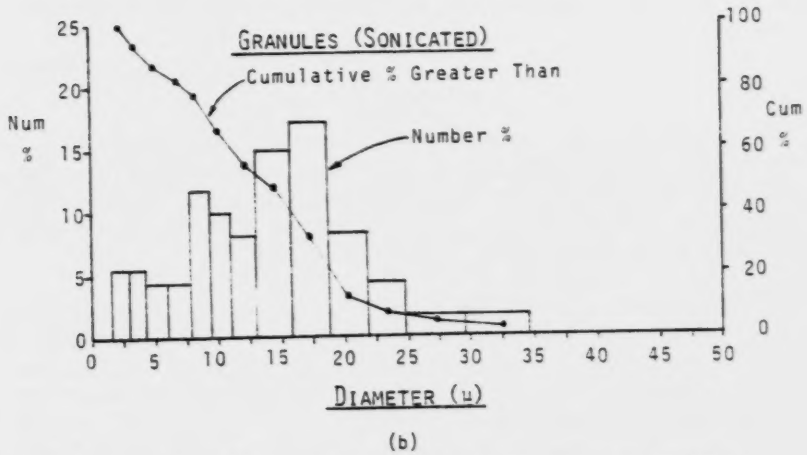

(b)

Figure 4-7. Graphic display of number count of $CaSO_3$ granular particles.
a) non-sonically dispersed preparation; Total count, 78; Count of Figure 3-5a.
b) sonically dispersed preparation; Total count, 43. Count of Figure 3-1a.

A typical example of platelets is shown in Figure 4-8a. The field is rather sparsely populated to avoid agglomerates. The sample, from an actual scrubber, was aspirated onto a Millipore filter substrate; it was not sonically dispersed and magnification is 200X. Figures 4-8b and 4-8c show sections of the same field at 400X and 800X magnification. Very few new particles were detected at the increased viewing power; certainly no vast number of small particles dominates the sample. Figure 4-9a represents the count of this crystal field. Very few extremely large (>40μ in width) particles were seen, and if the samples were handled with care, relatively few small broken pieces were observed.

A typical photograph of a sonicated sample is seen in Figure 4-10a. That sample, from the same batch as before (i.e., in Figure 4-8), was mounted as before and is shown at 200X magnification. Comparison photographs at 400X and 800X of part of the same field are in Figures 4-10b, and c, respectively. Typical of several other such microscopic enlargements of areas of photographs, very few particles were "missed" in the 200X photograph compared to the 800X photograph; see Table 4-1. Size measurements at 800X

TABLE 4-1. DETERMINATION OF FINE PARTICLES MISSED AT 200X MAGNIFICATION; OPTICAL MICROSCOPE

Sample	Total Particles Counted at 200X	Total <5μ Particles Counted at 200X	Number of <5μ Particles "Missed" in Box at 200X From 800X Photograph	By Extrapolation, Total Number of <5μ Particles in 200X Photograph	Percent Missed at 200X
Fig 4-8	47	14	1	4	8%
Fig 4-10	155	73	2	8	5%

compared to 200X were only slightly (~10%) more precise. Again, some of the smallest particles (specks) were later determined to be fly ash. Indeed, 30% of the particles are below 5μ (counting only small ones which show angularity - presumably therefore not fly ash). Again, the background appears to contain more "trash". Many of the smaller particles are angular, probably being "broken-off" chips. These particles, more common in sonicated samples, are somewhat thicker than the 1:30:45 relative dimensions; their calculated ESD will be perhaps a factor two too small.

4.3 SEM COUNTING

The scanning electron microscope produces much higher quality micrography, but of course it is much more expensive and time consuming. It was used primarily to check on the optical method. Significant differences were found. The optical microscope cannot be used to identify particles smaller than 2μ in width, and is somewhat questionable below for widths less than 4 or 5μ. Above that size, with proper technique, optical microscopy should be as accurate as SEM.

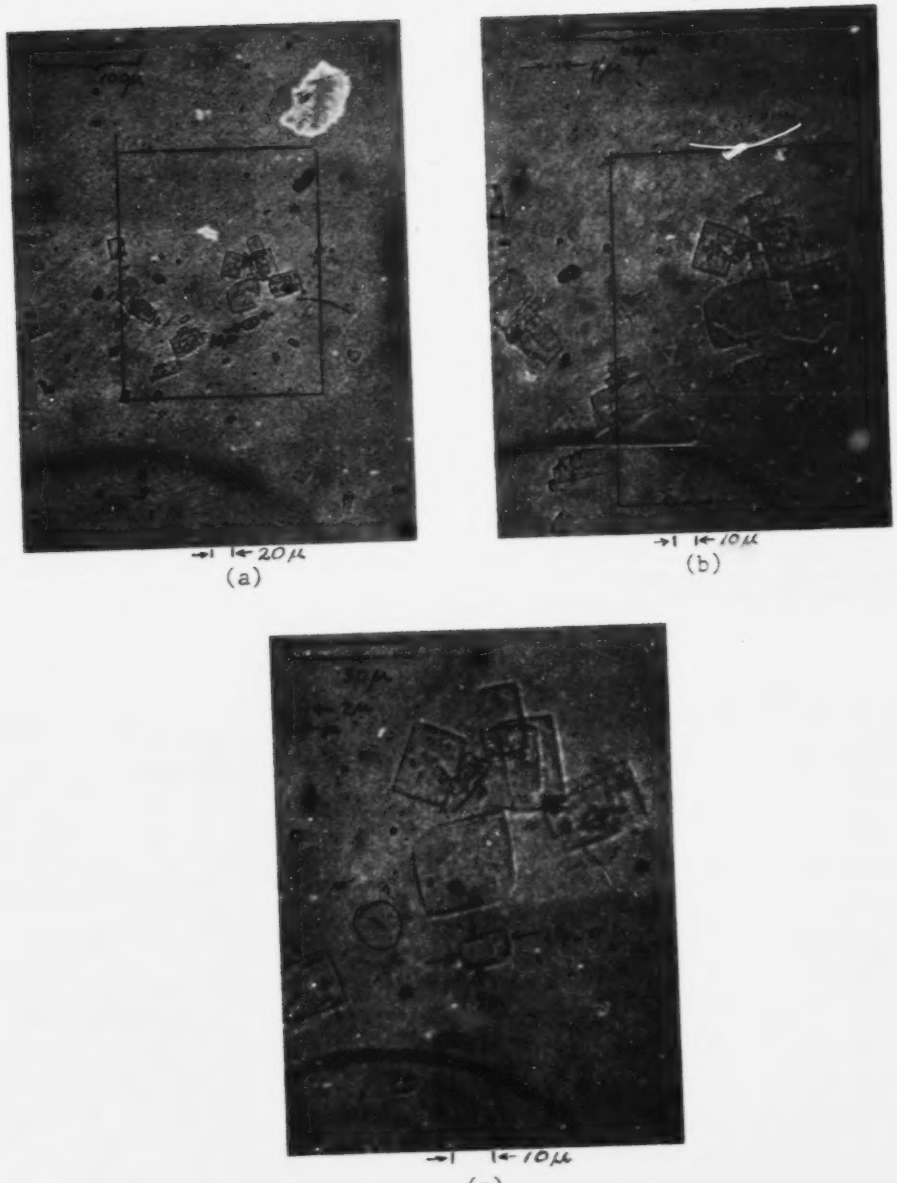

(a) (b) (c)

Figure 4-8. Optical photograph of $CaSO_3$ platelets.
The field chosen is sparsely populated to avoid agglomerates.
Not sonicated.
a) 200X
b) 400X, area of (a) in box
c) 800X, area of (b) in box
The count of (a) appears in Figure 4-9a.

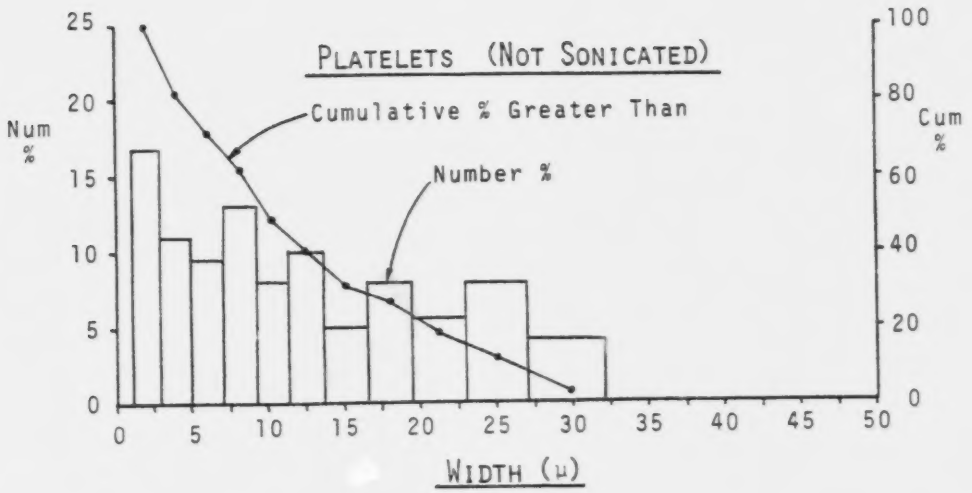

(a)

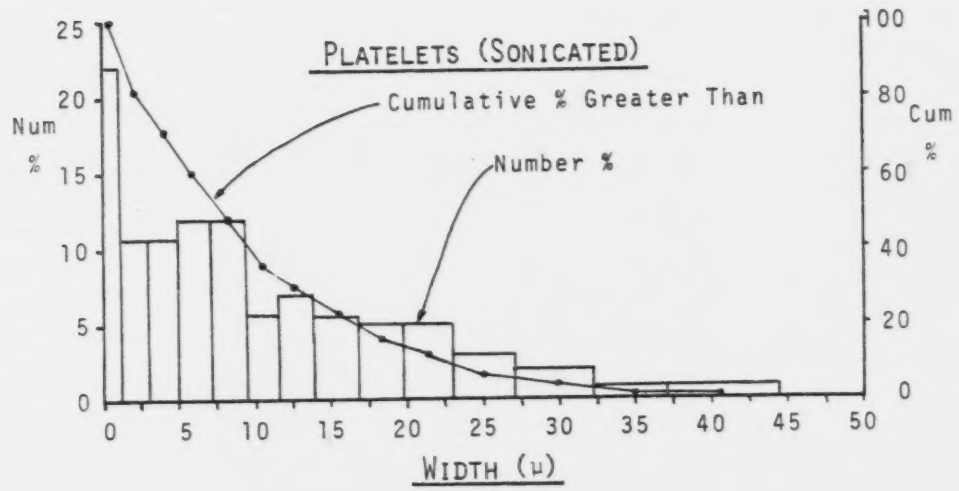

(b)

Figure 4-9. Graphic display of the number count of $CaSO_3$ platelet particles;

a) non-sonically dispersed sample; Total count, 47
Count of Figure 4-8a.
b) sonically dispersed sample; Total count, 166.
Count of Figure 4-10a.

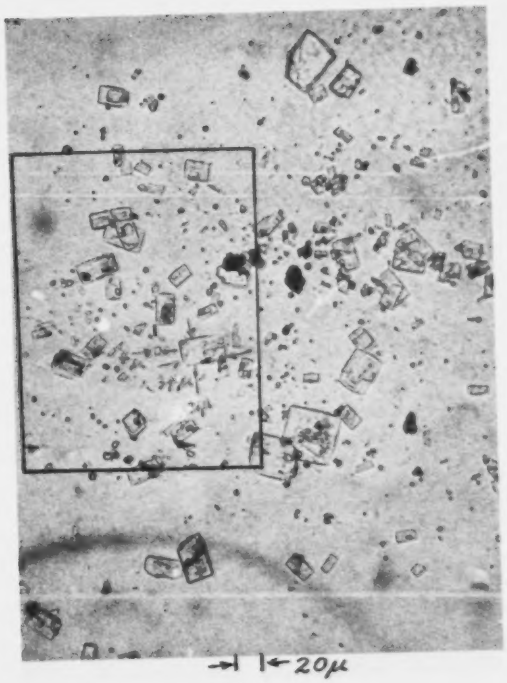

(a)

(b)

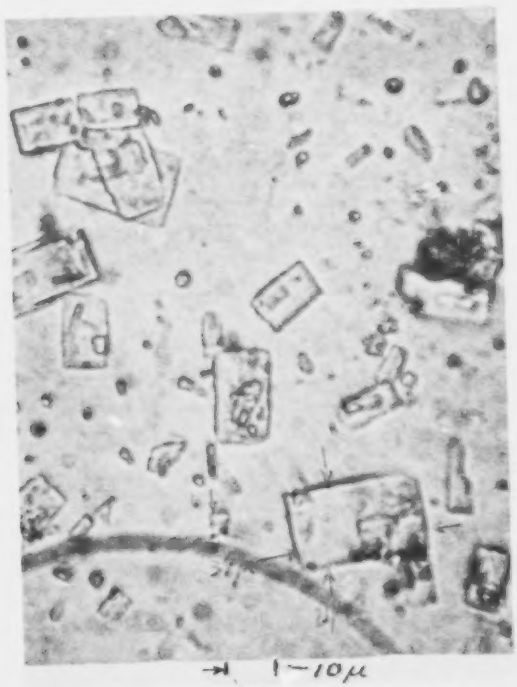

(c)

Figure 4-10. Optical photograph of $CaSO_3$ platelets. The sample has been ultrasonically dispersed.
a) 200X
b) 400X, area of (a) in box
c) 800X, area of (b) in box
The count of (a) appears in Figure 4-9b.

When the SEM is operated at 200X, the pictures are more clearly defined than with the optical microscope at a comparable magnification; see Figure 4-11. This is another photograph of $CaSO_3$ platelets from a full-size scrubber (also see Figure 4-2). In the preparation, the sample in Figure 4-2 was not ultrasonically dispersed; the sample in Figure 4-11 was. A comparison of the photos for the effects of sonication will be given after the counting is discussed; see Section 4.3.3.

4.3.1 Number Count

In either photograph, Figure 4-2 or 4-11, the left side is at about 200X magnification, and the cursor, enlarged on the right, is at about 1000X. A careful number count of the left sides was made and is graphically displayed in Figure 4-12. The number of smaller particles increases generally in an exponential fashion. However, when the 1000X cursor is carefully inspected, many particles (<1.5μ) are found that were not identified in the same area at 200X magnification. Some are particles deeply imbedded in the Millipore filter support; some are particles adhering to or growing out of the surface of larger crystals. Others are just too small to be defined as particles at 200X magnification. Table 4-2 gives the actual counting data on these photographs; see Table 4-1 for a comparison with optical microscopy.

TABLE 4-2. DETERMINATION OF FINE PARTICLES "MISSED" AT 200X MAGNIFICATION; SEM

Sample	Total Particles Counted at 200X	Total <1.5μ Particles Counted at 200X	Number of <1.5μ Particles Missed at 200X, From 1000X Cursor	By Extrapolation, Number of <1.5μ Particles Missed in Whole Photo	Fly Ash Particles Missed at 200X, From 1000X Cursor	By Extrapolation Number of Fly Ash Particles Missed in Whole Photo
Fig 4-2 (non-sonicated)	125	15	10	250	8	200
Fig 4-11 (sonicated)	152	27	20	500	8	200

The cursor covers only 1/25 of the area of the left side. As Table 4-2 shows, if the cursor area is considered to be typical, when the number of particles newly identified in it is multiplied by 25, an estimate of the small particles (<1.5μ) missed at 200X is obtained. This estimate shows that many more particles are being missed (small particles) than are being identified (all particles). Recall that the slurry was aspirated onto the filter without vacuum, so few particles are presumed to have been lost into the Millipore filter matrix. If these assumptions are approximately correct, then approximately 70% of the particles are smaller than 2μ (80% if fly ash is

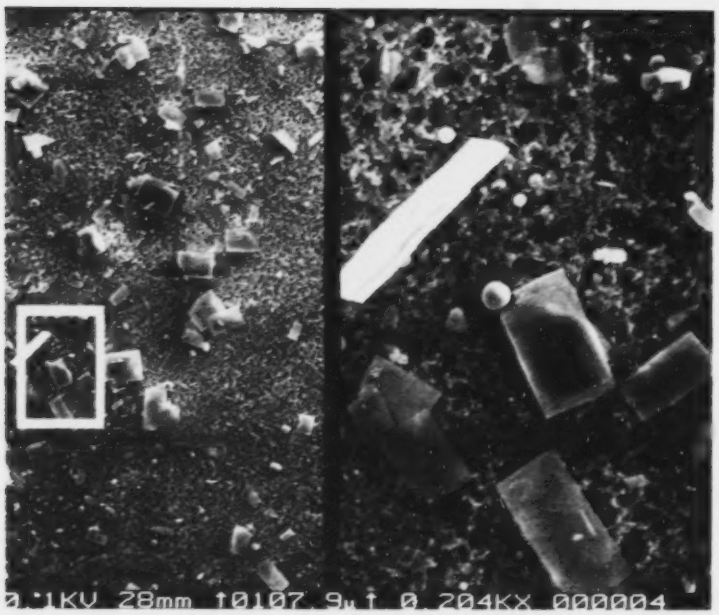

Figure 4-11. SEM photograph of sonically dispersed sample of $CaSO_3$ platelets; 204X. The cursor on the right is 5X the 204X magnification. Note that many of the "rectangular" platelets are erroded at the edges and corners.

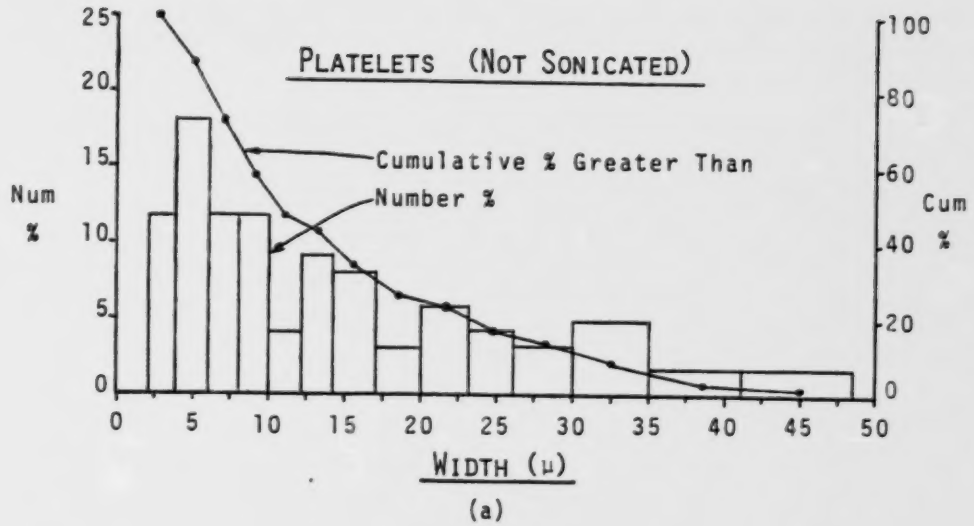

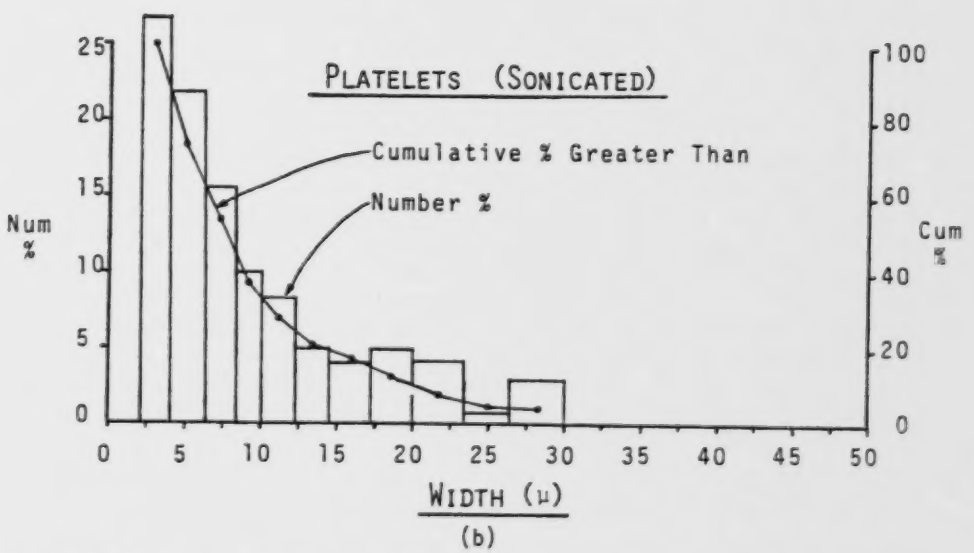

Figure 4-12. Graphical display of the visual count of SEM photo (200X) of platelets.
a) not sonically dispersed; Count of Figure 4-2; Total Count 125.
b) sonically dispersed; Count of Figure 4-11; Total Count 152. Note general shift of probability toward the smaller size range in sonicated sample.

included) in the non-sonicated sample and 80% (90% with fly ash) in the sonicated sample. This conclusion will be shown to be in reasonable agreement with the results of instrumental methods.

It is therefore clear that optical number counting is inaccurate below about 4μ for optical microscopes and below about 2μ for SEM (at 200X). If higher magnifications are used, optical methods lose resolution and few new, small particles are identified. For SEM the magnification can be increased with good resolution, but then the sample becomes so small that several fields of view are required for a representative sample. Such techniques should be fairly good for particles in the 4-8μ size range and quite accurate for larger sizes (assuming the other difficulties discussed earlier in this section can be overcome).

4.3.2 Volume Counting

If one casually glances at a 200X SEM photograph, either Figure 4-2 or 4-11, one does not see a preponderance of small particles. Rather the eye tends to see a volume count; that is, most of the volume (or mass) appears to be intermediate in size. Figure 4-13 gives a volume count of Figure 4-2 (also see Figure 4-12a for the number count), and the presentation satisfies the intuitive impression that one gets from viewing these photographs. The three large particles at the lower left in Figure 4-2 represent fully 30% of the volume of all $CaSO_3$ platelets in the picture. The vast numbers of fine particles occupy only a miniscule percentage of the volume.

Figure 4-13 shows that the particles smaller than 2μ account for only 0.013% of the volume. If the population of fines extrapolated from the cursor results is included (70% of the numbers), the small particles still occupy only 0.2% of the $CaSO_3$ volume. Inclusion of the estimated 200 fly ash particles raises the fines volume to 0.3%. Hence, the volume count, reflective of what the eye sees, is dominated by large particles. The number count, the data required by most mathematical models, is dominated by small particles. Numerical results, derived from volume count results via shape factors, may be inaccurate since the small particle region of the volume count is poorly determined. It is just this size region that will be most important in the number count.

4.3.3 Effect of Ultrasonic Dispersion

Ultrasonic dispersion, or sonication, is routinely used to break up agglomerates in samples for instrumental counting. It has been assumed that sonication does not damage the crystals. It may or may not dislodge crystals adhering to or growing out of larger crystals. These phenomena were investigated with the SEM. The effects of sonication on instrumental counts is discussed in Section 5.

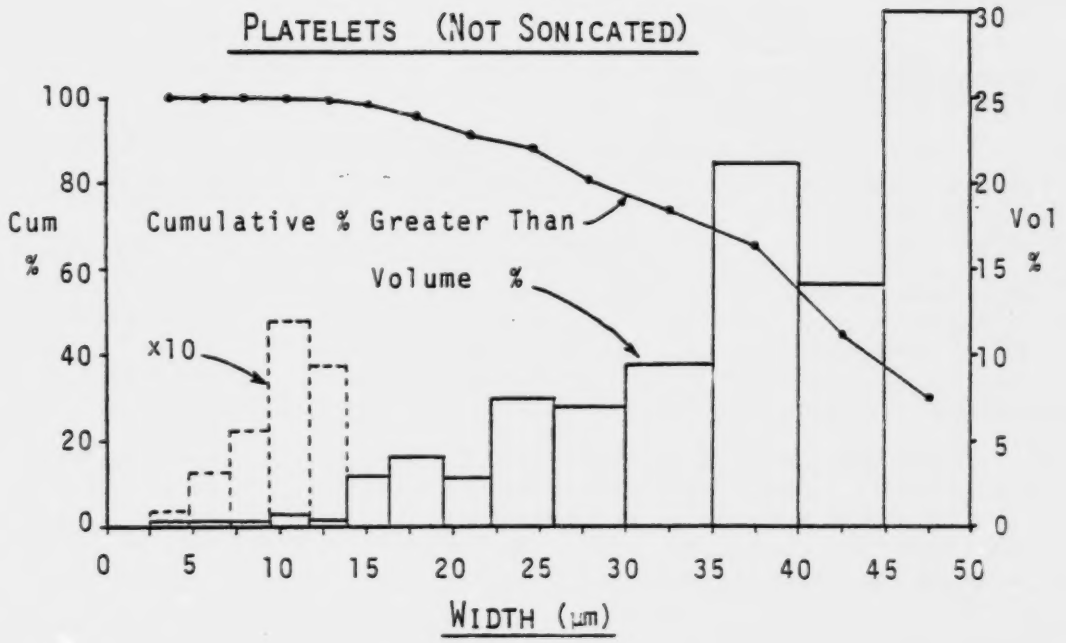

Figure 4-13. Graphical display of volume count calculated from number count given in Figure 4-12a.
Note the dramatic shift in the shape of the histogram from Figure 4-12a.

According to the limited number of SEM photographs used, it does appear that sonication reduces the size of $CaSO_3$ crystals. Figure 4-12 compares number counts of the same sample, one (a) prepared without ultrasonics and the other (b) prepared with the treatment. The sonicated sample does show a shift in the number percent count toward smaller sizes.

Two features also noted in the optical microscopic comparison are similarly found in these samples. First, very large particles are seen after sonication; see Figure 4-12a where a few particles were identified as large as 45μ wide. Secondly, many more smaller particles are seen; again see Figure 4-12 and compare the regions below 10μ.

Other samples that were sonically dispersed and photographed on the SEM showed a definite increase in the finer particles; see Figure 3-3 at 500X. For instance, 75% of the sonicated particles are at 9.0μ or smaller; the comparable figure was 54% for the nonsonicated sample. Again, no large particles (>30μ in width) are seen in this sonicated sample. The "gnawing" around the edges of the crystals due to sonication is well depicted in the 2500X cursor of Figure 3-3. It appears that sonic dispersion does alter the number count by breaking large particles and generating more smaller ones. As we shall see later, instrumental counting results generally show a smaller average size for the whole distribution after sonication.

No attempt was made to count granular crystals in SEM micrographs because it is impossible, for the purpose of identifying nucleation sites, to define what a particle is. Inspection of Figures 4-3 or 4-4 clearly shows what is present, but also dramatically illustrates the impossiblity of counting, let alone sizing.

SECTION 5

RESULTS OF INSTRUMENTAL METHODS

Instrumental particle sizing techniques have several distinct advantages over visual or manual counting methods. They are objective, fast, size or count large samples, and give reproducible results. However, they do not distinguish between different particle types in mixtures of particles. This includes the inability to differentiate large particles from agglomerates. They measure an effective spherical diameter and shape factors must be determined by other means if the true particle dimensions are sought. They measure a size distribution based on mass (or volume); this can be converted to a number distrubution. Finally, the particles must be immersed in a fluid.

5.1 COULTER COUNTER RESULTS

One of the primary objectives of this project was to determine the most suitable, reliable means to count particles by size. This includes an understanding of the reasons for discrepancies between optical and instrumental methods [1]. To this end, samples of $CaSO_3$ particles, both granules and platelets, were sieved, photographed and counted by the Coulter method. Identical samples were run with and without sonic dispersion. A complete compilation of results will be found in Appendix A.

Two presentations of the data are frequently used. The Coulter Counter actually measures a volume count, which can be converted to mass count if the particle density is known. The relative or percentage number size count may be obtained by dividing the number count in each size interval by the average particle volume for that size range. In most cases the number count will be given the Coulter Counter data processor. Thus a small volume of tiny particles can convert to a very large number of tiny particles. Nearly all the counts in this report show such a characteristic. For example, the data shown in Figure 5-1 (and included in Appendix A) show a volume maximum at 5.5μ with very little volume below 2μ. Still, the number count increases nearly monotonically as the particles diminish in size. Figure 5-2 is a logarithmic plot (where a true exponential curve plots as a straight line) of the relative number count. These plots are linear over most regions and indicate that the population is behaving exponentially. The only exceptions appear to be in ranges that were enhanced by sieving or transition regions between true exponential regions.

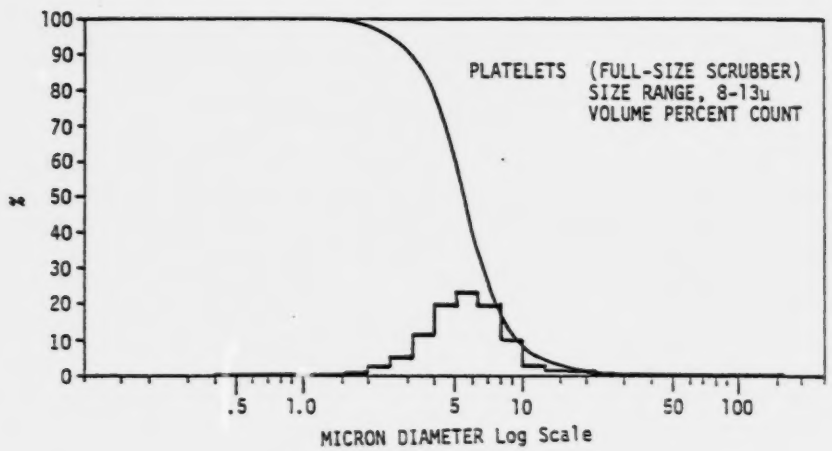

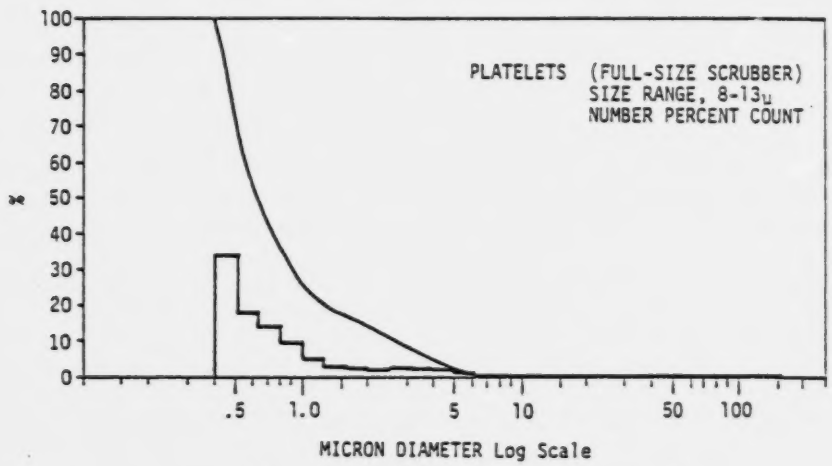

Figure 5-1. Platelets in size range 8-13μ.
Top: Volume Count
Bottom: Number Count

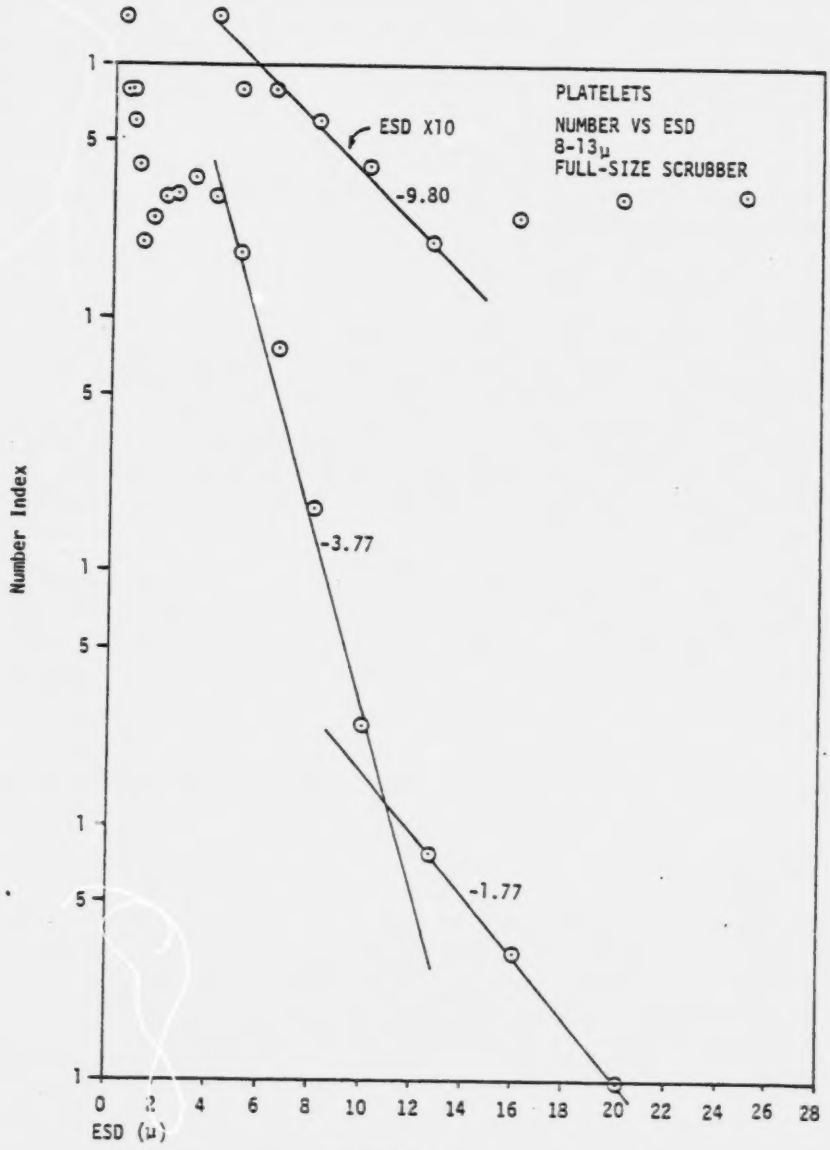

Figure 5-2. Logarithmic display of number count of platelets in the 8-13 μm size range. See Figure 5-1b.

Most crystal growth theories (1, 2) predict that the number of particles in a size range is (negatively) proportional to the size. That is:

$$\frac{dN}{dL} \alpha - N \text{ or } \frac{dN}{dL} = -\sigma N \qquad (5\text{-}1)$$

where σ is the constant of proportionality and L is a one dimensional crystal size parameter (like equivalent spherical diameter). The solution of this differential equation is:

$$N = Ae^{-\sigma L} \text{ or } \ln N = -\sigma L + \text{Constant} \qquad (5\text{-}2)$$

Thus, a plot of ln N versus L will be a straight line with a slope of $-\sigma$. Speculation on the relation of σ to the crystal growth mechanism may be found in either of the two references at the beginning of this paragraph and will not be specifically addressed here. However, the occurrence of several straight line regions in the present data indicates that different mechanisms are in effect in different size ranges. It is proposed that the steep slopes (about -10) below 2μ found in particles from production-line scrubbers are due to fly ash.

The occurrence of several straight lines on the log-population plot indicates that multimodal population control mechanisms are operative. For the purposes of mathematically modeling a scrubber, it may be necessary to deal with a compound exponential population equation of the form:

$$N = Ae^{-\alpha L} + Be^{-\beta L} + Ce^{-\delta L} + \ldots \qquad (5\text{-}3)$$

where different ranges are dominated by different terms in this type of equation.

5.1.1 Granules

The principal goal of this project was to determine a method that could satisfactorily size a population of sludge crystals. Instrumental counting of the granular $CaSO_3$ crystals appears to be an acceptable solution. To this end, laboratory grown $CaSO_3$ crystals were seived into size ranges, photographed and counted visually and instrumentally. The micrographs of the three size ranges, >20μ, 13-20μ, and 8-13μ appear in Figure 5-3. The volume-per-size-range count, an analysis that reflects what the eye sees, agrees fairly well with the trend expected from sieves. The maximum population location, the mode, appears to be in best agreement with the expectations from the sieving (see Table 5-1). Appendix A is a complete exhibit of the data.

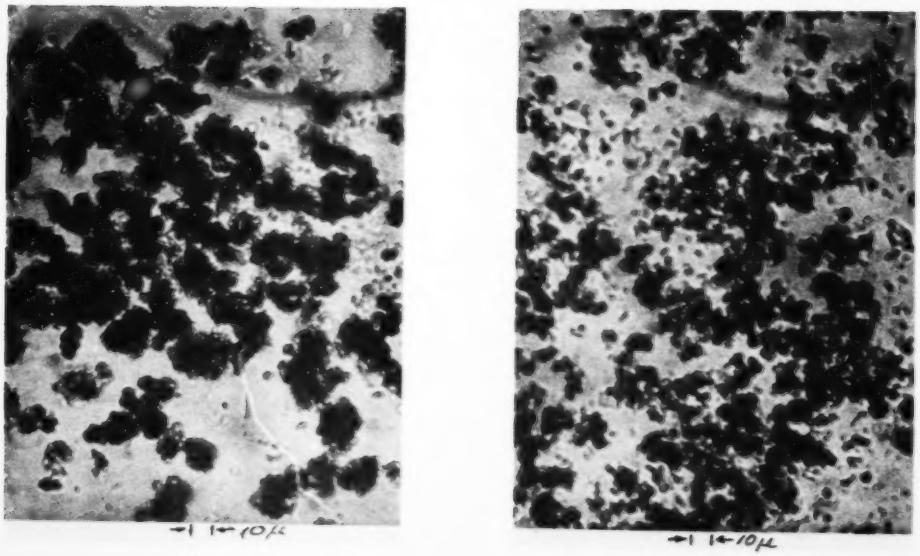

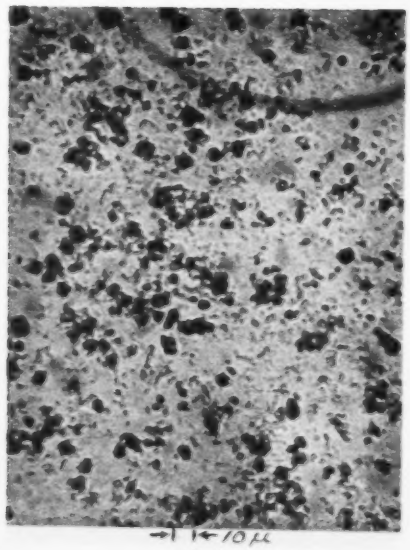

Figure 5-3. Optical micrographs showing results of sieving $CaSO_3$ granules. Magnification at 400X. General size differences are readily apparent. Instrumental counts of these batches are included in Appendix A.
a) >20μ batch
b) 13-20μ batch
c) 8-13μ batch

TABLE 5-1. ESTIMATES OF CENTRAL TENDANCY FOR VOLUME COUNT ON GRANULES OF $CaSO_3$ BY THE COULTER METHOD

Particle Size (μ)	Sonic Dispersion	Geometrical Mean (μ)	Median (μ)	Mode (μ)	Standard Deviation
>20	No	13.58	16.77	20.34	2.10
>20	Yes	11.40	13.82	15.34	2.28
13-20	No	7.31	7.77	12.06	2.47
8-13	No	8.13	8.54	7.55	2.50

Since these samples were sieved from successive batches of laboratory grown $CaSO_3$ crystals, they contained no fly ash. However, regardless of the amount of washing, a large number of small particles were always present, see Figure 5-3. Although the volume count paralleled expectations from sieving, in the number count the fine particles still dominated. The sieves effectively segregated larger particles but appear to have had little effect on the smaller particles.

For the batches of larger sized particles, one would expect the number count to begin at a greater ESD. For the batches of smaller sized particles, the percentage count should begin at smaller diameters, but then increase more quickly (steeper slope). These expectations are met for these data, see Figures A-2, A-4, A-6, A-8 and Table 5-2. The 8-13μ batch shows some irregularities from the others in that it appears to be bi-modal over this range. The average of the two slopes is probably a more representative figure (see Table 5-2).

TABLE 5-2. LOG-NUMBER SLOPES OF SIEVED GRANULES

Particle Size (μ)	Sonic Dispersion	Slope >5μ	Slope <5μ
>20	No	- 0.82	-3.62
>20	Yes	- 1.00	-3.98
13-20	No	- 1.38	-3.30
8-13	No	-1.83 (-1.42)*	-10.90

*The average of the two slopes for particles >5μ.

The 8-13μ fraction also has an inordinately steep slope in the below 5μ region, where all other samples were quite similar. But otherwise, the Coulter results agree with the expectations from the sieving preparation.

The Coulter data are reported in terms of equivalent spherical diameter. The granules appear to be approximately spherical; see Figure 4-4. The ESD's observed should give good relative size correlations. However, granules are not solid. Since the Counter method actually measures the true volume displaced, it effectively reports a solid sphere. Thus, the apparent optical size concentration maximum in the micrographs may be larger than the volume concentration maximum determined by the Coulter method. A direct comparison is not possible since the void volume of the granules is difficult to estimate; again refer to Figure 4-4.

Finally, the behavior of the log-number curve for the >20μ granule fraction should be discussed: refer to Figure A-6. The plateau region around 8μ is inconsistent with any exponential population mechanism. Similar behavior is seen in some of the platelet fractions, and mechanisms may be operable that result in such populations (e.g., new particles formed exclusively from attrition). However, recall that each batch was sieved into size fractions, and one might therefore expect a maximum in the number count curve. In practice this was seldom found. Generally, the sieving effectively sized larger particles only, and the smaller particles were always present in each size fraction. The 20μ sieve was the easiest to use (less clogging), and the plateau may be a reflection of that efficiency.

5.1.2 Platelets - Volume Count

In general the Coulter results on $CaSO_3$ platelets were less reliable from one sample to another than were the granular particle counts. Two sets of samples were run, one from a full-scale, operative scrubber (fly ash included) and another from a model or pilot scrubber (no fly ash). Both sets were sieved consecutively into several fractions, photographed and Coulter counted.

The first set run was $CaSO_3$ scrubber sludge from a full-scale scrubber. Figure 5-4 shows three photos of the size ranges after sieving; 13-20μ, 8-13μ, and 5-8μ. Again, the seiving appears to be effective on the larger particles. The 13-20μ fraction shows no particles whose width is greater than 20μ, and only a few crystals whose length is slightly greater than 20μ. The 8-13μ fraction micrograph similarly shows no particles wider than 10μ and none longer than 16μ; however, the background shows an unusually large number of smaller spherical particles, probably fly ash. The 5-8μ fraction shows many fine particles but none whose width exceeds 8μ. These surveys of size maxima cover at least three micrographs similar to those in Figure 5-4 for each size fraction. In summary, the pictures indicate that the sieving has restricted the size of the large particles to the expected range.

Again, the volume count reflects the trends expected from sieving; see Table 5-3.

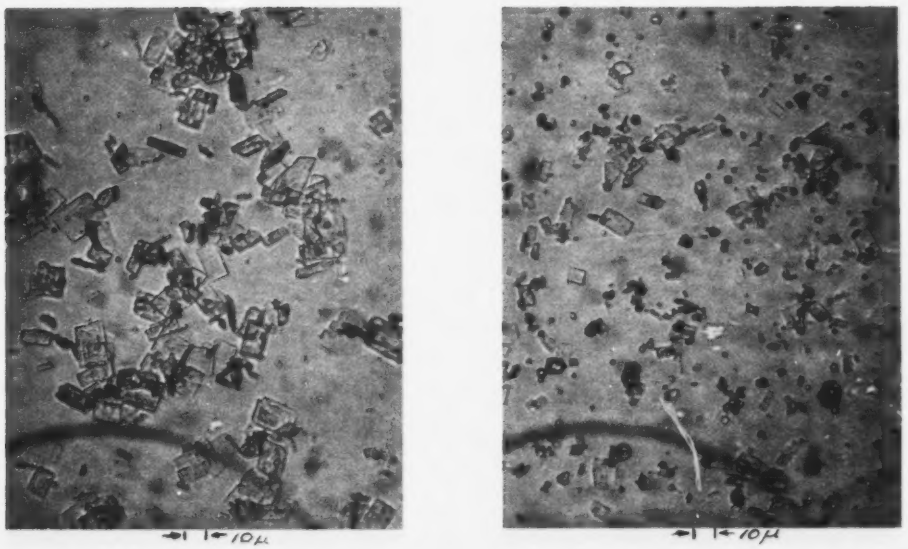

(a) (b)

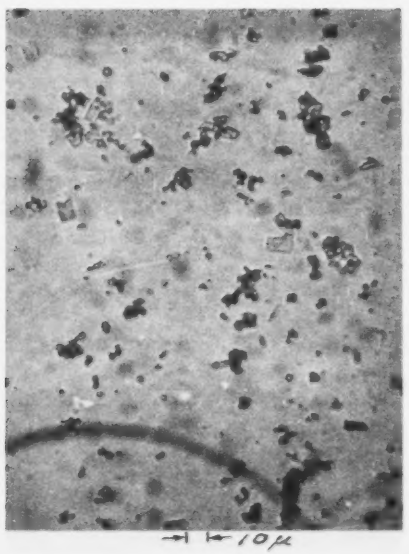

(c)

Figure 5-4. Optical micrograph showing results of sieving of $CaSO_3$ platelets from a full-scale scrubber. Magnification at 400X. General size differences are readily apparent. Instrumental counts of these batches are included in Appendix A.
a) 13-20μ batch
b) 8-13μ batch
c) 5-8μ batch

TABLE 5-3. ESTIMATES FOR CENTRAL TENDANCY FOR VOLUME COUNT ON $CaSO_3$ PLATELETS BY THE COULTER METHOD FOR FULL SCALE SCRUBBER

Particle Size (μ)	Sonic Dispersion	Geometrical Mean (μ)	Median (μ)	Mode (μ)	Standard Deviation
13-20	No	8.05	8.38	10.08	2.28
13-20	Yes	7.73	8.18	7.64	2.37
8-13	No	5.48	5.52	5.66	1.66
5-8	No	5.18	4.45	3.56	2.27

The complete population curves are in Appendix A, Figures A-9, A-11, A-13, A-15. These data appear quite regular and show no exceptions to the expected trends. The small standard deviation of the 8-13μ batch means that the volume count is bunched rather tightly around the average value (or most common value [mode]), about 5.5μ; see Figure A-13a. The micrograph shows most of the crystals to have one of their dimensions (length or width) within this range; however, the thickness is impossible to determine with the optical microscope. Other studies have judged the thickness to be about one-twentieth of the width (1); SEM work has shown that some are much thinner. An estimate can be made from the Coulter analysis of the sieving product if one assumes 10.5μ as an average rectangular dimension for the 8-13μ batch determined by microscopy. Recall that the Coulter data are reported in terms of equivalent spherical diameters. For this case ESD = 2R = 5.5μ (from Table 5-3):

$$t \times 10.5 \times 10.5 = \frac{4}{3} \pi \, (R = 2.75)^3 \qquad (5\text{-}2a)$$

$$t \times (110.25) = 4.189 \, (20.797) \qquad (5\text{-}2b)$$

$$t = 0.790\mu \qquad (5\text{-}2c)$$

for a width-to-thickness (t) ratio of something like:

$$w/t = 10.5/0.790 = 13.3. \qquad (5\text{-}3)$$

The earlier studies [1] assumed an average crystal geometry of 1:20:30, so the agreement for thickness estimates is only approximate. With w/t = 13.3, the predicted ESD based on the sieving would be: 13-20μ batch, 8.65μ; 8-13μ batch (as calculated above), 5.5μ; and, the 5-8μ batch, 3.41μ. The agreement to the geometrical mean size for each batch (Table 5-3) is only fair; about the same can be said for agreement with the median and mode.

The second set of data resulted from a similar procedure run with $CaSO_3$ platelets from a pilot scrubber at RTP; there was no fly ash in the sample. Again the samples were sieved, photographed and Coulter counted. The results are given in Table 5-4.

TABLE 5-4. ESTIMATES FOR CENTRAL TENDANCY FOR VOLUME COUNT ON $CaSO_3$ PLATELETS BY THE COULTER METHOD FOR PILOT SCALE SCRUBBER.

Particle Size (μ)	Sonic Dispersion	Geometrical Mean (μ)	Median (μ)	Mode (μ)	Standard Deviation
>20	No	15.56	16.55	17.38	1.69
13-20	No	10.23	10.22	9.97	1.59
13-20	Yes	11.57	11.23	10.16	1.70
8-13	No	9.31	10.01	13.25	2.26

Once again, the sieving appears to have successfully restricted the sizes of the larger particles; see Figure 5-5. In the greater-than-20μ batch, many smaller particles are seen, but particles whose width is 18 to 20μ are common (Figure 5-5a). The 13-20μ batch is clearly made up of smaller particles. From several micrographs, no particle was seen larger than 15μ in length. Nor was any particle seen greater than 13μ in width; see Figure 5-5b. The 8-13μ batch was not as well size resolved; it did contain particles as large as 15μ in length as well as many smaller particles. The trends in Table 5-4 reflect the population trends in the micrographs, except for the mode in the 8-13μ sample.

The oddity in these data is the instrumentally determined increase in size after sonic dispersion. No other example showed this behavior. The operator insisted that the probability of a "switch" in the data between the 13-20μ sonicated and nonsonicated samples is very small. The increase in mean size after sonication, especially when a decrease is expected, is outside the expected range of technique variability. The result stands without explanation.

However, another problem is introduced by these data. They do not compare well with the other sieved platelet Coulter counts. A comparison of the micrographs of similarly sieved samples (Figure 5-4a, b with Figures 5-5b, c, respectively) suggest that the pilot scale scrubber samples appear under the microscope to be slightly larger. Yet the Coulter data statistical figures are from 25 to over 200 percent larger for the second set of batches. Again, this discrepancy is not believed to be instrumental

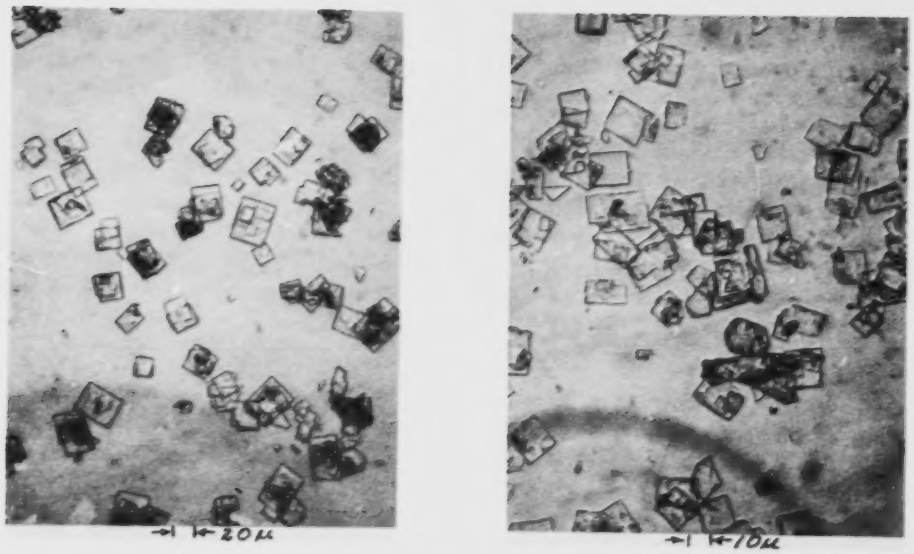

(a) (b)

(c)

Figure 5-5. Optical micrograph showing results of sieving of $CaSO_3$ platelets from an RTP pilot scrubber. Magnification at 200X for (a), 400X for (b) and (c). General size differences are readily apparent. Instrumental counts of these batches are included in Appendix A.
a) >20μ batch
b) 13-20μ batch
c) 8-13μ batch

error. It is not possible to account for these consistently higher results for the second set of samples (i.e., those from RTP) by comparison of length and width measurements of the two samples. This observation led to a more careful analysis of the third dimension, thickness.

Measuring the thickness of thin platelets, even on the SEM, is difficult. The best example obtained was shown in Figure 4-6. Here the edges appear at oblique angles. A great range of thicknesses is seen. The largest crystal in the center appears to be rather thick on the left end (as viewed in this micrograph). This end is the result of breakage, and the resulting cross-section is clearly exposed. However, the other end appears to taper off and is comparatively quite thin. The back length edge may also be thin, suggesting an "airfoil" shape. The crystal immediately below it clearly is thicker in the center than towards its edges. Thus, the crystals appear to fatten in the middle where the crystal-molecular alignment forces are greatest. If breakage occurs, then all width-to-thickness ratios are lost. In this picture alone, the width-to-thickness ratio range from 12:1 to 54:1.

Hence, the thickness of a platelet, necessary for comparing the optically determined length and width size with the instrumentally reported equivalent spherical diameter, are optically indeterminable. The width to thickness ratio can vary over a range of at least four, and that ratio is probably quite dependent upon the crystal history. That is, growth time and conditions, in addition to breakage, very likely significantly influence crystal geometry.

The constant size differential between the two sets of samples that were Coulter counted is probably real. The thickness variation may account for the reported differences in the equivalent spherical diameters.

Optical inspection for volume determination is consequently nearly impossible. The Coulter method is probably the best available to volume-size crystals of this type. Still, results like the sonicated sample in Table 5-4 caution against overconfidence even with this method.

5.1.3 Platelets - Number Count

The Coulter method measures the volume of particles in a size range. For the purposes of mathematical scrubber models (1), the number-per-size-range is needed. The volume percent in a size range may be converted to a number percent by dividing by the volume. For large particles (>20μ), the differences are not great. But for very small particles, the change in distribution is enormous. A tiny volume percent may account for 40% of the number count. The volume and number percent histograms are given for eight samples in Appendix A.

The number counts are generally exponential-type population curves. They are best analyzed as log plots where true exponential behavior results in straight lines.

At larger particle sizes (ESD >10μ, which corresponds to a width at least >20μ), all four of the sieved platelet batches show nearly identical behavior; see Table 5-5.

TABLE 5-5. LOG-NUMBER SLOPES OF SIEVED PLATELETS FROM FULL-SIZE SCRUBBER

Particle Size (μ)	Sonic Dispersion	>10μ	Slope Near 5μ	Slope <2μ
13-20	No	-1.38	-2.00	-4.92
13-20	Yes	-1.31	-1.91	-5.33
8-13	No	-1.17	-3.77	-9.80
5-8	No	-1.29	-4.20	-1.47

Again, these four platelet samples were sieved consecutively from a full-size scrubber's sludge, and they therefore contain fly ash.

Since no particles were optically observed in the large size range (>10μ), these counts probably represent agglomerates or coincidence counts. The curve in this region is a very good exponential, and either of the above explanations should produce such behavior. That is, the occurrence of agglomerates or coincidence counts is proportional to the total number of particles.

If the sieves do "knock-out" larger particles but discriminate little among the smaller particles, percent number count curves should be steeper for the smaller size range batches. This trend was indeed observed for these platelet samples; see Table 5-5. The intermediate size region, near 5μ ESD or 10-15μ platelet width, is the region of sieving size discrimination. While the volume count showed some differences between sonicated and non-sonicated samples, the number count gives almost identical results for both. The number count for the smaller size batches would also be expected to begin at smaller sizes. This behavior is observed for the 5-8μ and 8-13μ ranges; for the 13-20μ range, the slope differs so little from the larger particle slope (coincidence event background) that it is difficult to tell where the straight line for the intermediate sized particles begins, and the behavior may well be within expected bounds. Refer to Figures A-10 and A-12 in Appendix A.

At smaller size ranges (<5μ ESD), nonexponential behavior is encountered. Both the 5-8μ and 8-13μ range platelet batches show local maxima. Presumably the number count would sharply decline if not for the very steep

slopes found below 2μ. Similar transition regions (between good straight line-exponential regions) are also found in the number count displays of the pilot scrubber platelets.

Regions of no increase or an actual decrease in the number count indicate that the exponential-type growth mechanism is no longer operative. These regions exist in most number-count curves, including the optical count curves. Apparently, a preferred size is generated by certain mechanisms. In fact, the 2-10μ region of Figure A-14 appears Gaussian shaped; i.e., of the general form,

$$e^{-\alpha(x-x_o)^2}. \qquad (5\text{-}4)$$

Breakage of certain size particles or clustering or agglomeration of particles governed by some size preferential mechanism could result in such a curve, but verification of such speculation is beyond the scope of this project.

The very steep curve below 1.5μ in Figure A-14 is probably due to fly ash. Indeed, the SEM reveals large numbers of spherical fly ash particles below 2μ. Thus, in full-scale scrubbers, the fly ash will probably mask the population statistics of $CaSO_3$ platelets below 2μ. In both platelet and granular samples grown in laboratory and pilot plant scrubbers, where no fly ash is present, such steep slopes are not seen.

The $CaSO_3$ platelets grown in the RTP pilot plant scrubber exhibit sizing statistics similar to those of the platelets from a full-scale scrubber. Two or three regions show rather straight lines on log paper, usually with a plateau region in the intermediate size range (5-10μ ESP). These transition regions are not believed to be due to sieving because: (1) the sieving did not effect smaller size ranges, and (2) the largest size batch of the full-size scrubber sample which physically sieved most efficiently, showed no plateau. Again, certain of the curves display Gaussian characteristics (see Figures A-18, A-20). The slopes of the rather well defined straight lines are given in Table 5-6.

TABLE 5-6. LOG-NUMBER SLOPES OF SIEVED PLATELETS FROM RTP PILOT SCRUBBER

Particle Size (μ)	Sonic Dispersion	Slope >10μ	Slope ∿3μ	Slope <2μ
>20	No	-0.90	-1.86	-4.49
13-20	No	-1.87	∿0	-6.12
13-20	Yes	-1.46	∿0	-10.30
8-13	No	-1.28	-3.60	-6.19

The slopes of the 13-20μ samples near 3μ were nearly flat, but no straight line could be defined.

In conclusion, it seems that the Coulter method gives internally consistent results when analyzing samples from a common source. Comparison between samples with different histories may not be valid. Volume-counts tend to reflect what the eye "sees," but number-counts are more useful for mathemetical models. The number-count curves tend to give straight lines when plotted on log paper, an indication of exponential population behavior. The plateau regions unpredictably encountered in sieved samples may or may not reflect the efficiency of the sieving. Certainly, they are nonexponential regions; in fact, several curves appear rather Gaussian. Population regulating processes appear to be multimodal and no easily identifiable mechanisms suggest themselves. Possibly, the steep slopes (<-10) below 2μ are due to fly ash which can be seen in SEM photos adhering to larger particles.

SECTION 6

NUCLEATION STUDIES

6.1 INTRODUCTION

One of the secondary goals of this project was to study $CaSO_3$ crystal nucleation and growth processes in order to produce a higher quality sludge; quality here, is defined by settling rate and dewaterability. $CaSO_3$ platelets certainly settle faster than granules [1] and they generally dewater better. The goal then was to study certain process variables to see which ones had an effect on crystal growth and nucleation.

Ottmers, et al. [3] have reported that $CaSO_3$ supersaturation levels of up to 3 resulted in no spontaneous precipitation. They did note that precipitation below this level could be induced by seeding.

In laboratory batch crystallization experiments without seeding it was not possible to produce platelets. Granules invariably formed independent of solution temperature, solution pH, stirring rate, and changes in $CaSO_3$ concentration. Occasionally, a few platelets formed initially, but after more crystal growth, granules were found to be in the vast majority.

Growth of platelets was possible only with platelet seeding. Slightly supersaturated $CaSO_3$ solutions, when seeded with platelets, did yield predominately platelets. Granule seeds produced only granules. If supersaturation ever passed a level where nucleation became spontaneous (about 3 times saturation) or the $CaSO_3$ concentration changed rapidly enough for one to notice momentary changes in opacity, granules were the result. Hence, only platelet seeding followed by slow growth (over periods of hours) would produce platelets.

It was found that solution pH was critical in crystal nucleation. At concentrations of Ca^{++} and $SO_3^{=}$ around .01 to .05M*, no precipitate spontaneously formed at pH lower than 4.6. Solid $CaSO_3$ dissolved in aqueous solutions below about 3.2 pH. Equilibrium calculations indicate that bisulfite, HSO_3^-, will predominate below about pH 3.5 for this concentration range. It was much simpler to initiate crystallization in a controlled manner by pH variation rather than by direct concentration variation.

*M represents molar concentration. Technically the concentration should be a formality, but molarity is far more commonly used.

$SO_4^=$ is always a contaminant in $SO_3^=$ studies. Extreme measures, like double gaseous barrier insulation, are necessary to prevent oxidation of the sulfite. For example, purified N_2 still contains enough O_2 so that if laboratory solutions are purged with N_2, some of the $SO_3^=$ will be oxidized in the process. At temperatures above 40°C oxidation is quite rapid (seconds) and complete to the extent possible, limited only by available O_2. Also, $CaSO_4$ is relatively water insoluble and pH levels below 2 are required to dissolve it (to HSO_4^-).

6.2 GRANULES

Little need be said about nucleation mechanics and kinetics for granules. Any rapidly precipitating solution will produce granules. Without seeding they form more readily than do platelets. As the concentration (or pH) of a non-precipitating saturated solution is increased, the driving force toward crystallization increases. At some point the first crystals will form as tiny platelets. But by that time the supersaturation levels are high enough to cause incipient nucleation and growth, and many platelets grow out of the original crystal in a rapid, haphazard fashion. An irreversible change takes place. The product is a nearly spherical ball consisting of hundreds of platelets cocked at all angles. Figure 4-4 shows an excellent sample of this type of granular growth.

Thus, granules are really spheres of multiple platelets jammed awkwardly together. This morphology encloses many dead spaces and results in voids between the platelets. This accounts for the lower dry density of the granules (1.25), compared to the platelets (1.39), and explains why they are difficult to dewater. The entropy of the granules is apparently greater than that of the platelet crystals, and granules are the morphology of choice for rapid crystallization and growth.

Granules grown at higher supersaturation levels (hence, more rapid growth) appeared under the microscope to be slightly smaller than more slowly grown granules. In any case, the spheres formed were 2-10μ in diameter, with a much tighter range in any one sample; see Figure 6-1. The spheres immediately formed into agglomerations.

Due to their much larger surface area, the granules dissolved more rapidly in acid than did platelets. When granules and platelets formed a mixed population and mild acid (pH 3) was added, the granules quickly broke up into hundreds of tiny platelets which subsequently quickly dissolved. Meanwhile, nearby platelets were more resistant to dissolution. In a mixture of granules and platelets, it is possible to dissolve nearly all the granules before dissolving very many platelets. This process is probably what happens in a SO_2 scrubber tower where the return tower make-up liquors still contain many calcium sulfite crystals. In the tower they are briefly exposed to the acidic environment created by the dissolved SO_2. The SO_2 contactor may be working as a fines destruction device, operating principally on the granules, and contributing greatly to the production of platelets as the final dominant product form.

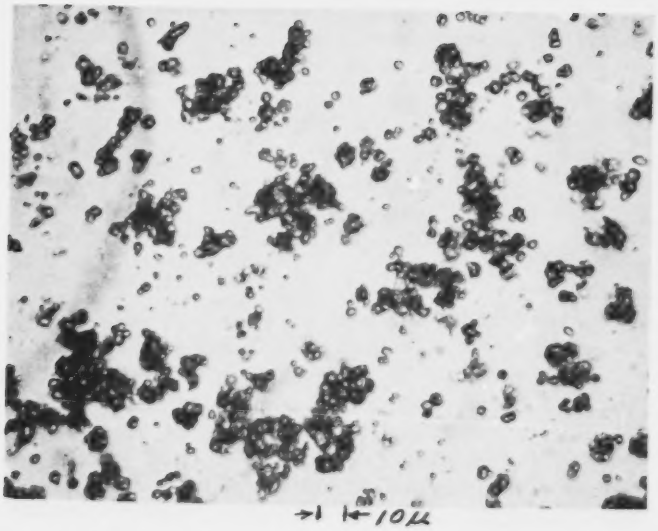

Figure 6-1. Optical micrograph of granules grown from seeded supersaturated $CaSO_3$ solutions. Note the size uniformity and agglomeration.

6.3 PLATELETS

In batch preparations, platelets could be induced only by seeding with other platelets. Stirring speed and temperature had no apparent effect (i.e., under microscopic examination) upon the size or type of crystals formed. The concentration of Ca^{++} and $SO_3^{=}$ were the principal determining factors. As was mentioned earlier, it was found to be easier to control the $SO_3^{=}$ concentration by varying the pH ($H^+ + SO_3^{=} \rightleftarrows HSO_3^-$) than by adding $SO_3^{=}$.

As the pH of solutions at about .04M Ca^{++} and $SO_3^{=}$ was slowly increased by the addition of aqueous NaOH, crystals formed spontaneously at a pH of about 4.8. If NaOH addition was stopped, more crystals continued to form (invariably granules), and the pH fell back (in several hours) to a value of about 3.5. In more concentrated solutions, spontaneous crystallization began at lower pH; for example, at .2M in Ca^{++} and $SO_3^{=}$, cloudiness appeared at pH 4.2. Temperatures differences between 0^oC and 60^oC had no noticeable effect on the pH at which spontaneous crystallization occurred.

A solution of .04M $CaSO_3$ at a pH of 4.5 without seeds would set for days with no crystallization, indicating that the threshold for spontaneous nucleation had not been crossed. Thus, nucleation experiments were carried out by adjusting, from below, the pH of a .04M solution to pH 4.5. Seed crystals were added and the container was sealed and allowed to stand at constant temperature for 16 hours. Crystals formed in the first few hours and further standing past 16 hours did not appear to have any effect. Temperature ranges of 0^oC to 60^oC also appeared to make little difference. All examinations were made with the optical microscope.

Seed crystals were sieved into different size batches. The amount of seed crystals added varied between 1 and 10 percent of the final product, again resulting in little apparent difference. No matter what size range was used for seed or how much seeding was used, the products looked very much alike in size; see Figure 6-2. The crystals seemed to grow to a certain surface area in size and few larger platelets were observed. That is, at some point the preferential growth coordinate becomes the thickness. This maximum area was typically 200-400μ^2 (e.g., 15 x 20μ or 18 x 18μ) for these growth experiments; again see Figure 6-2. Apparently, in spite of ample opportunity, under these conditions larger crystals rarely form. There was little chance for mechanical breakage; the few smaller, irregular crystal fragments seen confirmed this.

The size distribution of the laboratory grown samples showed an inordinately large percentage of certain large crystals; in fact, they looked more like the sieved sample (where one size range predominates) than a random sample. Recall that the seed crystals were only about 5% of the final crystal mass. A similar frequent size was seen in scrubber samples as well. The maximum predomonant size there was somewhat larger, up to 800μ^2, although

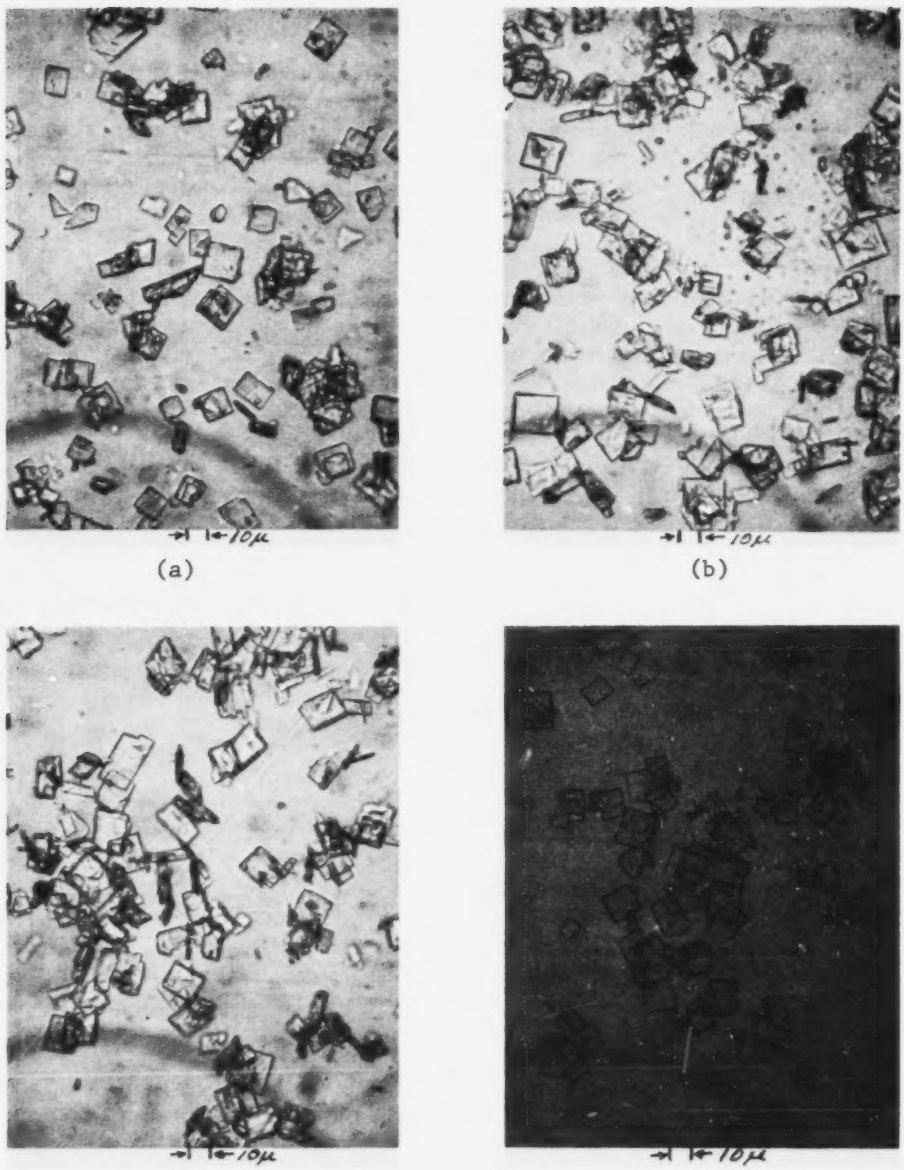

Figure 6-2. Product platelets from different seeding growth conditions.
a) sieved seed crystals, 13-20μ
b) product grown from 13-20μ seed at 0°C, pH 4.5 → 3.42; 5% seed
c) product grown from 13-20μ seed at 25°C, pH 4.5 → 3.42; 5% seed
d) product grown from 13-20μ seed at 25°C, pH 4.65 → 4.20; 1% seed

a few crystals as large as 1500μ^2 have been seen. Although time and conditions were available for "extremely" large crystals to form, none were seen. The constancy in size of the largest crystals in a batch, and more approximately from one batch to another, suggests that some growth limiting process (at least in area) appears to be operative.

There are many other variables that will affect crystal growth. The total ionic concentration or a host of surfactants are two known factors that can drastically alter crystal growth patterns. At one point in this work, buffers were used to maintain a constant pH during growth. However, the total ionic concentration was considerably different with the buffer, and a completely new crystal geometry resulted. This points to another potentially fertile area of research for improving the quality of sludge. Time and resources did not permit more extensive studies in this area.

SECTION 7

DISCUSSION OF RESULTS

7.1 SUMMARY OF VISUAL SIZING METHODOLOGY

The specifics of counting from photographs have been dealt with in earlier sections. This section will compare alternate visual methods of counting and arrive at more generalized conclusions.

Conventional optical microscopes are adequate for identifying and counting particles as small as a few microns. There may be problems of preparation, mounting or defining the particles or their geometry, but they are inherent to any type of microscopy. Depending somewhat on shape, particles below 4 or 5 microns are less well resolved in shape and size and a few are hidden or simply missed. For particles below 2 microns in size, optical microscopy is simply inadequate for size counting. All other methods indciate that large numbers of micron and submicron particles are missed under the best of optical conditions.

The counting of particles seen in optical micrographs is slow, tedious and discretionary. The problems of preparation, mounting and definition of particles mentioned in the previous paragraph are not to be casually disregarded. They may be, in fact, insurmountable as is the case for $CaSO_3$ granules. Increased magnification by immersion techniques allows only a slightly improved resolution of the particles. But the higher the magnification, the smaller the field of view and the smaller the sample per field of view. Indeed, if all other difficulties can be tolerably overcome, the size of the sample that can be reasonably counted may still be far smaller than is desirable. In the end, the trade-off between magnification and the size of the sample counted must be suited to the objective.

The problem of sample size is even more acute for SEM studies. The magnification is readily available and the resolution is high, but to generate a reliable result would require many micrographs and much counting. The technique is also costly and more time consuming than optical microscopy. And the mounting and preparation difficulties may be even more complex for SEM.

In conclusion, microscopy appears to be a poor technique for size counting. The optical microscope is relatively quick and easy. It is a good way to survey the sample for general characteristics such as general size, different morphologies and varieties of particles present. It is even an acceptable method for obtaining an approximate count for particles larger than 5 microns.

The SEM, although slower and more costly, provides more detail. It is best used to survey the small particle range (below 5 microns) and to more carefully determine crystal shape, especially for complex particles.

The combined optical count method could never be used for routine examination. Its chief use would be to complement instrumental methods being used or considered. Also, the instrumental methods do not directly distinguish between different types of particles, and for that reason a quick, optical inspection of any sample is advisable.

The count of $CaSO_3$ platelets (both with and without sonic dispersion) for several fields is shown in Figure 7-1. In this figure, the large numbers of submicron particles believed to be missed on 200X to 400X magnification micrographs have not been included. If they were, the number of particles below 2μ would vastly increase; however, the total volume of fine particles would remain below 1%. This total sample represents 766 particles counted, a number large enough to have some statistical credibility. The shape of the curve is in general agreement with instrumental counts discussed in Section 3.

7.2 COMPARISON OF VISUAL AND INSTRUMENTAL RESULTS

Some comparisons between visual and instrumental methods were included in Sections 4 and 5. There, a discussion of sizing involved reference to all possible techniques. The result of that comparison was that very little about the particle volume for platelets can be discerned using optical techniques. The platelet thickness varies widely, and the statistical averages resulting from instrumental counting are deceptively simplistic. That is, the clean, numerical results belie the complexities involved in size-counting a crystal distribution.

Because the thickness of platelets appears to have a broad range and cannot be measured optically, visual sizing (to volume) is nearly fruitless. For granules, even the definition of a particle is nearly impossible, and visual counting is impractical. Optical inspections can tell if all the particles are of the same general morphology and substance--information not readily available from instrumental methods. Visual methods could be useful for gross size approximations of similar samples. For example, the differences between the sieved samples were readily apparent at 200X using an optical microscope in transmission.

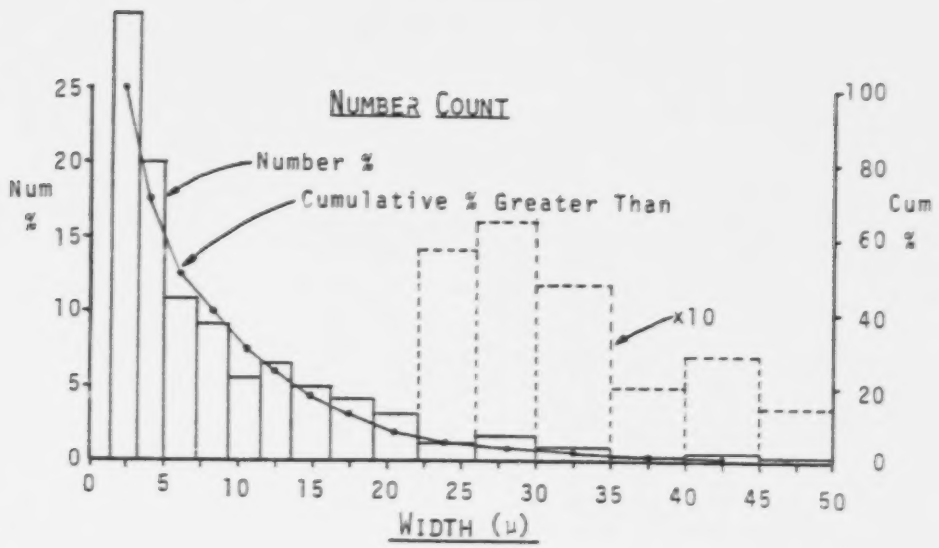

(a)

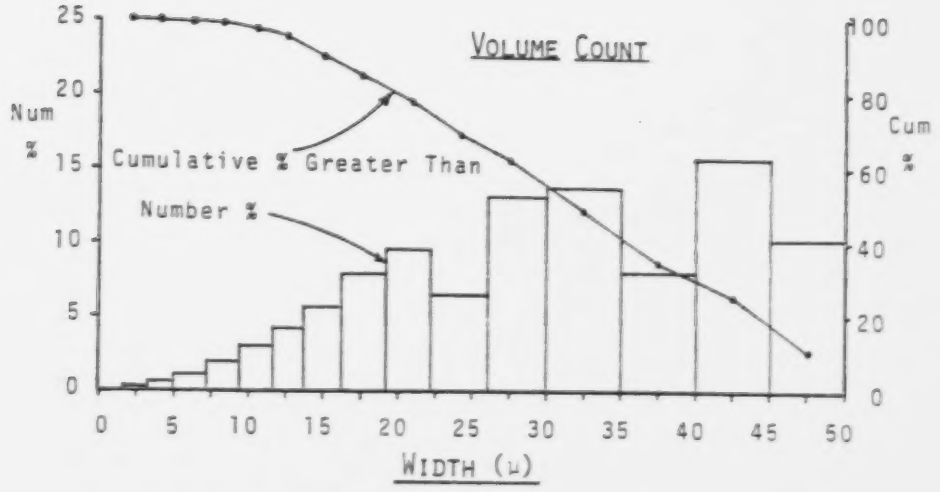

(b)

Figure 7-1. Graphical display of composite SEM counting (combined sonicated and non-sonicated counts).
a) number-count
b) calculated corresponding volume count

The SEM confirms that the thickness will vary even in the same batch of crystals. This may be due to different growth patterns, different histories or breakage. But the SEM is not a practical way to size a group of crystals. Optical microscopy is easier and less expensive than SEM and adequate for cursory inspection, but it is tedious and inherently subject to error. Neither method would be practical for a large amount of counting.

The Coulter method (and presumably sedimentation techniques) indiscriminately counts large numbers of particles. It is less subject to the vagaries of preparation. However, it is not free of inconsistencies, particularly in the volume-count statistics. A method that seems to give some order to the data is to plot the log of the number-count versus size; straight lines usually result. What an exponential growth population means is not within the scope of this work, but the result is in the form required by the mathematical model.

The granular $CaSO_3$ particle sizing results from the Coulter method appear fairly regular and straight-forward. However, for the purposes of the mathematical model, this approach may be misleading. The SEM shows the "particles" to actually be clusters of thin platelets growing radially out of nucleation centers. The number of individual crystals or nucleation events is undefinable. And, as with platelets, agglomerations are always present but to an undeterminable extent. Thus, although the granular sizing results seems to be internally consistent, their true meaning is uncertain.

One of the purposes of this project was to determine the best way to size-count particles and to make that information compatible with the mathematical modeling presented elsewhere [1]. The Coulter method is clearly the best choice to that end. It should be very good for particles with similar histories, such as repeated samples from a pilot scrubber. Optical or SEM inspection from time to time is strongly advised to determine generalized geometry and the presence of foreign particles. The visual inspection would be particularly necessary on a full-scale scrubber to check for limestone build-up or fly ash, either of which can significantly distort the Coulter results.

7.3 NUCLEATION

The nucleation studies showed that the pH is a very critical parameter in regulating the crystal growth. Platelets can grow only slowly and with seeding; granules are the fast-growth morphology. Among the other factors affecting growth patterns which may be operative in scrubbers, the total ionic strength of the solution appears to be most influential.

The nucleation studies support the conclusion reached elsewhere that at first growth occurs preferentially along the length and width coordinates; later, after a size is reached which depends upon solution conditions to some extent, the crystals thicken in the middle. Further growth appears to occur primarily in thickness. Thus, nucleation studies also support the conclusion reached elsewhere that judging crystal size by looking at the platelet area is ill-advised.

SECTION 8

REFERENCES

1. Phillips, J. L., et al., "Development of a Mathematical Basis for Relating Sludge Properties to FGD-Scrubber Operating Variables." EPA-600/7-78-072 (NTIS PB281582), April 1978, (Radian Corporation). EPA Project Officer: Robert H. Borgwardt.

2. Randolph, Alan D. and Maurice A. Larson, "Theory of Particulate Processes. Analysis and Techniques of Continuous Crystallization." New York, Academic, 1971.

3. Ottmers, D. Jr., et al., "A Theoretical and Experimental Study of the Lime/Limestone Wet Scrubbing Process." EPA-650/2-75-006, (NTIS PB 243399), December 1974, (Radian Corporation). EPA Project Officer: Julian W. Jones.

APPENDIX A

INSTRUMENTAL DATA

Some of the raw data, along with an alternate presentation, are collected in this appendix to avoid discontinuity in the body of the report. The odd-numbered figures display some raw data as received from Coulter Electronics which did the analysis. The subsequent even-numbered figure is a logarithmic plot of the number count for that sample. On these plots are given the slopes for each straight line segment that is reasonably well defined. All sizes in this appendix are in equivalent spherical diameters (ESD) in microns (μm).

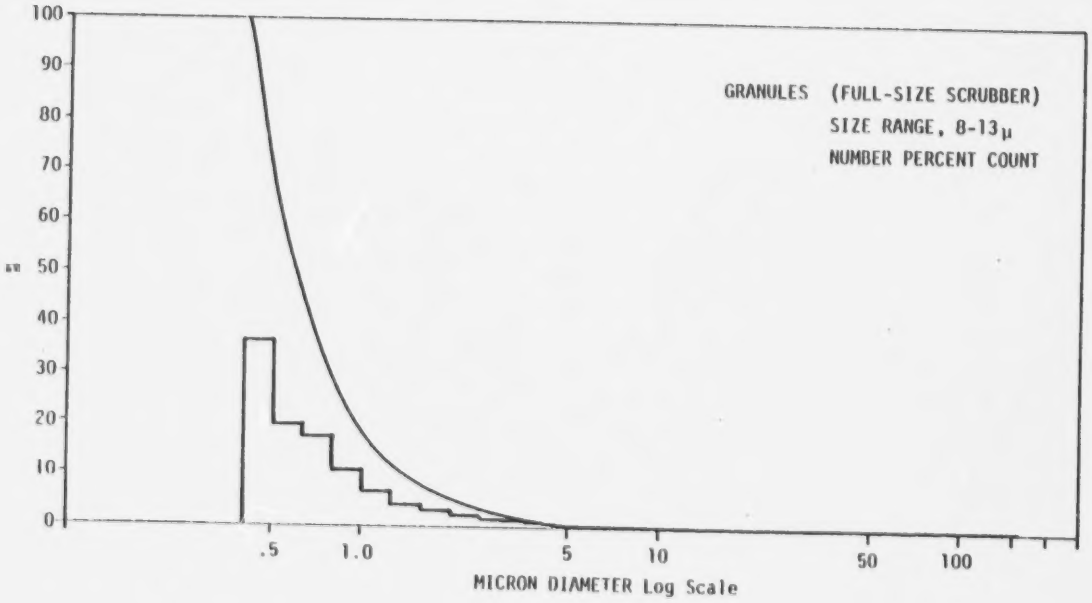

Figure A-1. Granules in size range 8-13μ; number count.

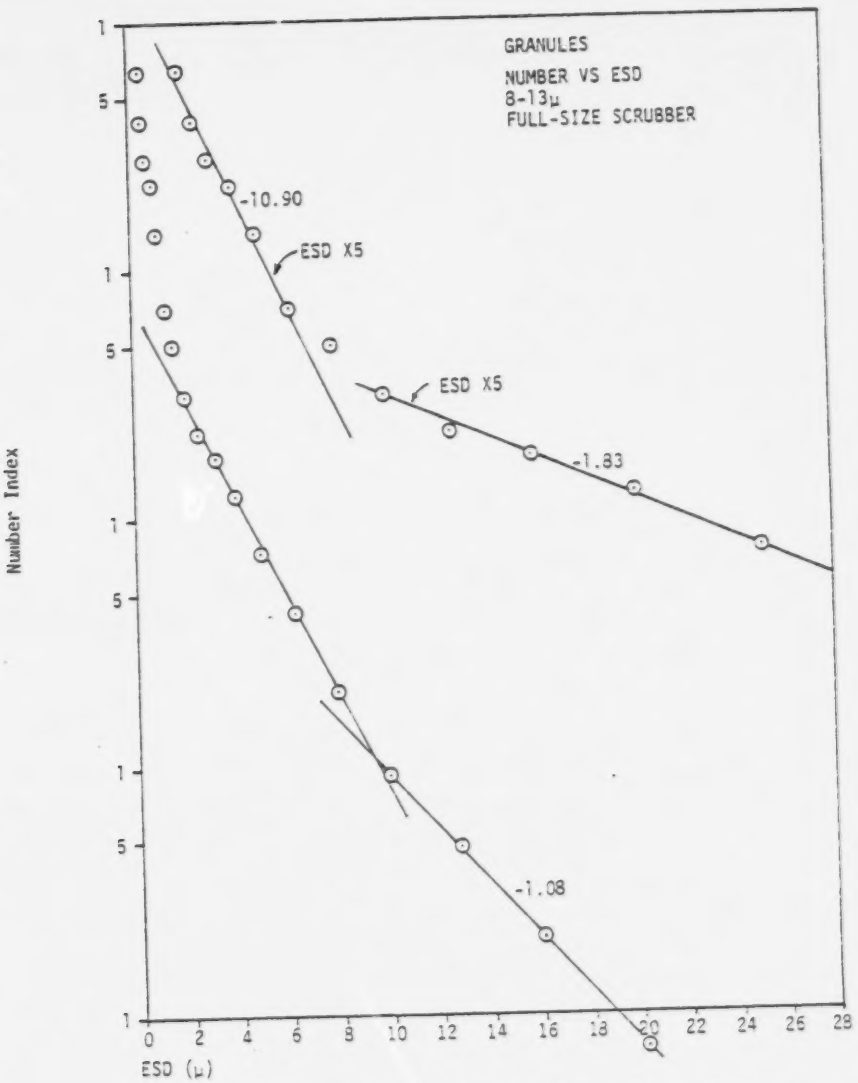

Figure A-2. Logarithmic display of number count in Figure A-1.

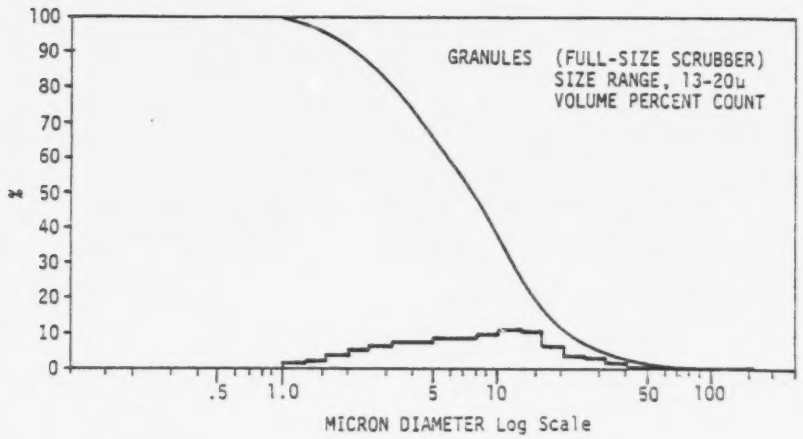

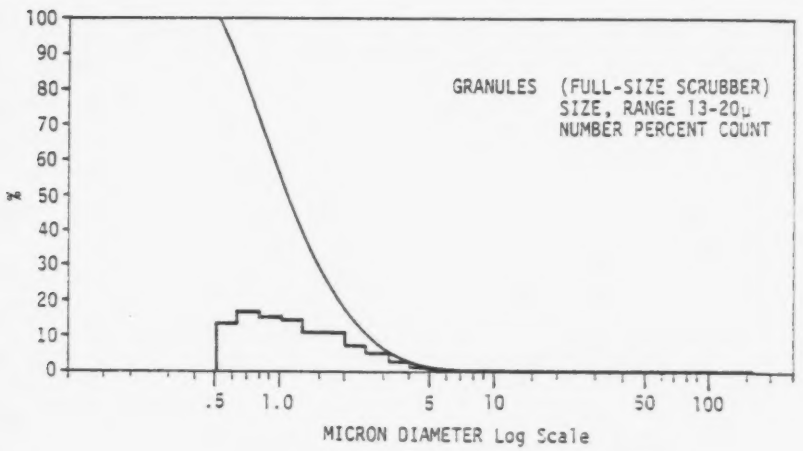

Figure A-3. Granules in size range 13-20u.
Top: Volume Count
Bottom: Number Count

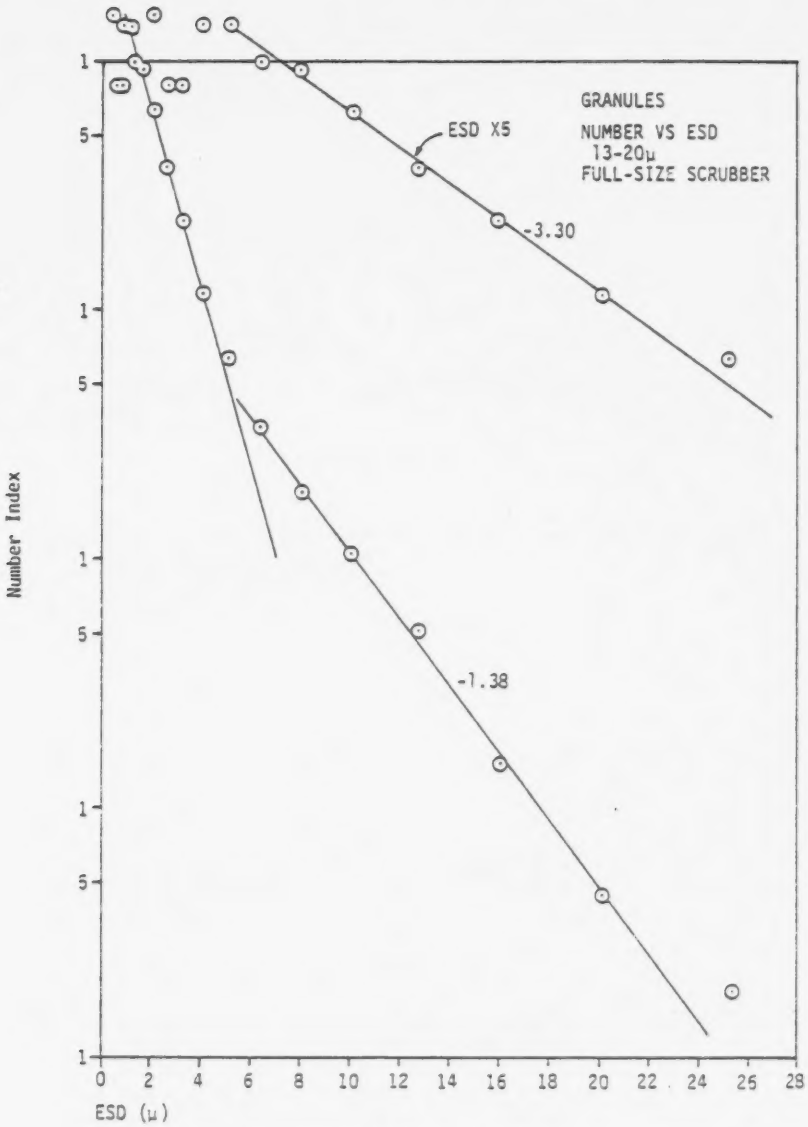

Figure A-4. Logarithmic display of number count in Figure A-3.

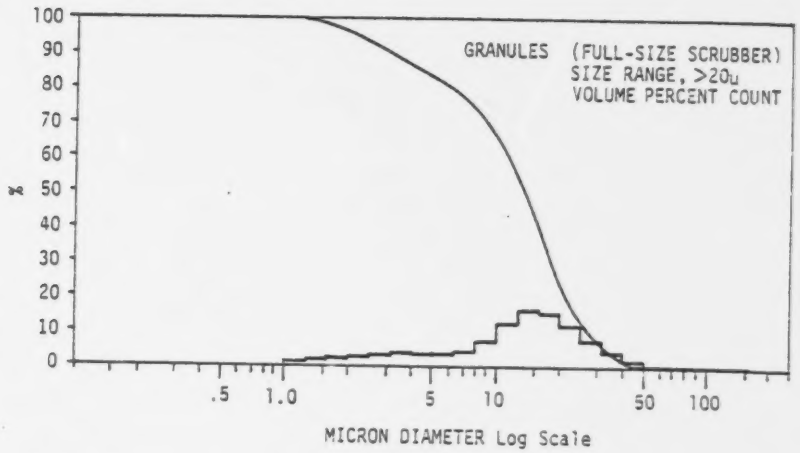

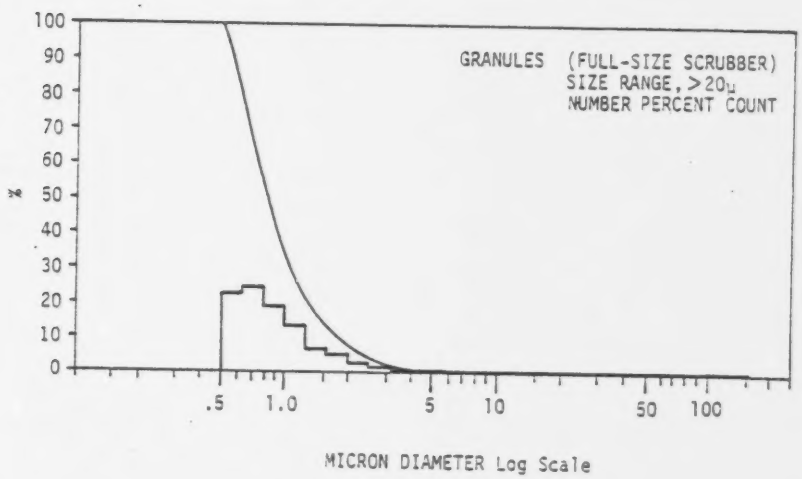

Figure A-5. Granules in size range >20μ; not sonicated.
Top: Volume Count
Bottom: Number Count

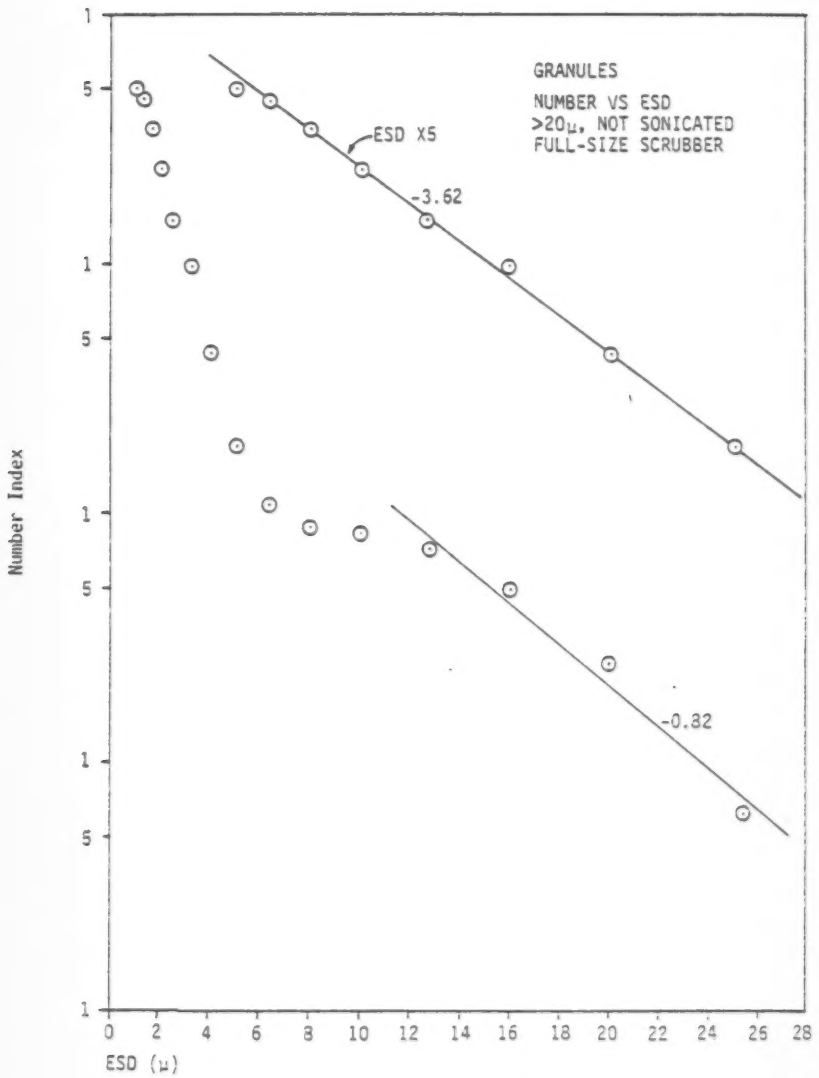

Figure A-6. Logarithmic display of number count in Figure A-5.

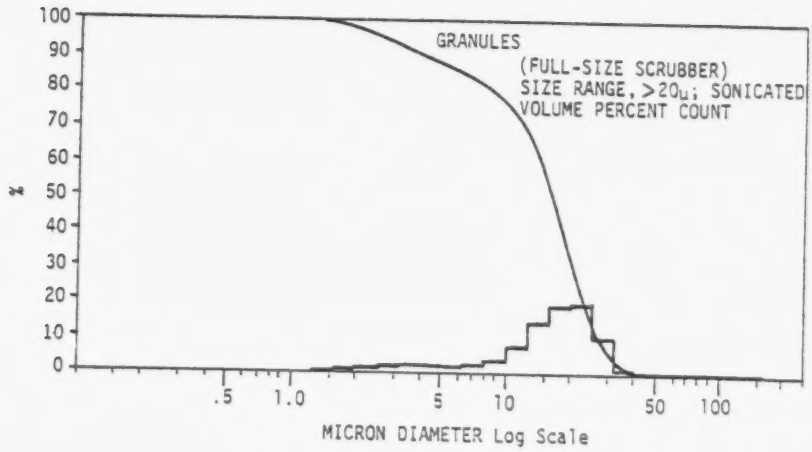

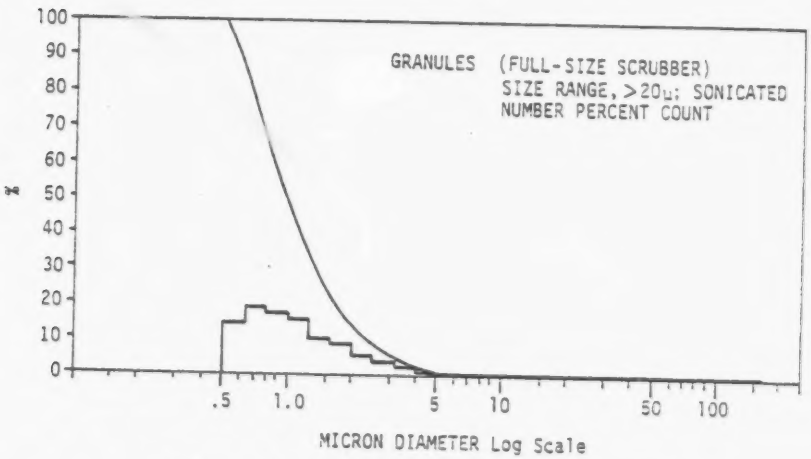

Figure A-7. Granules in size range >20μ; sonicated.
Top: Volume Count
Bottom: Number Count

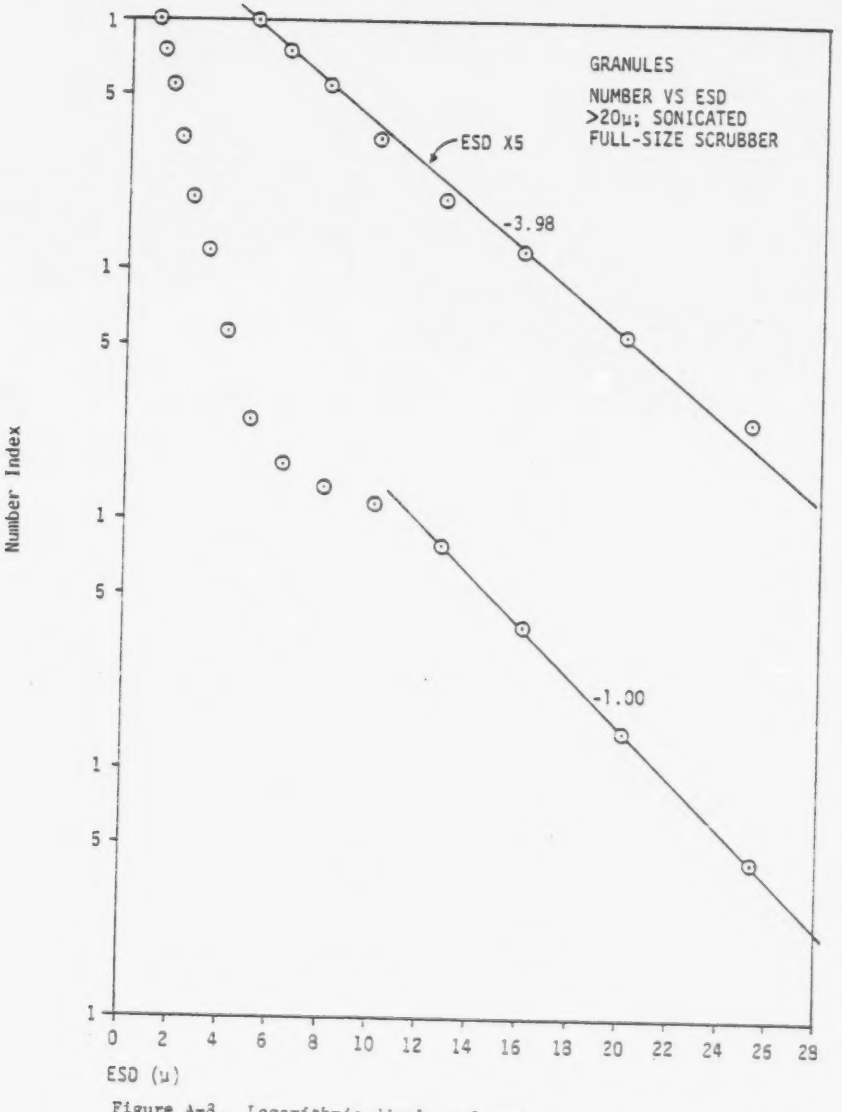

Figure A-8. Logarithmic display of number count in Figure A-7.

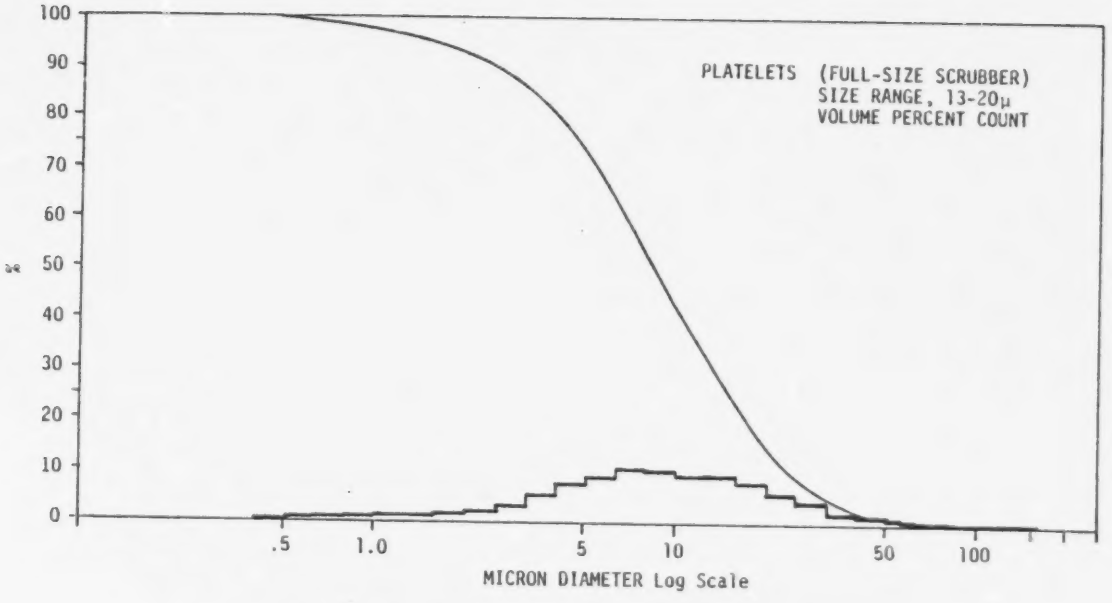

Figure A-9. Platelets in size range 13-20μ; not sonicated. Volume Count.

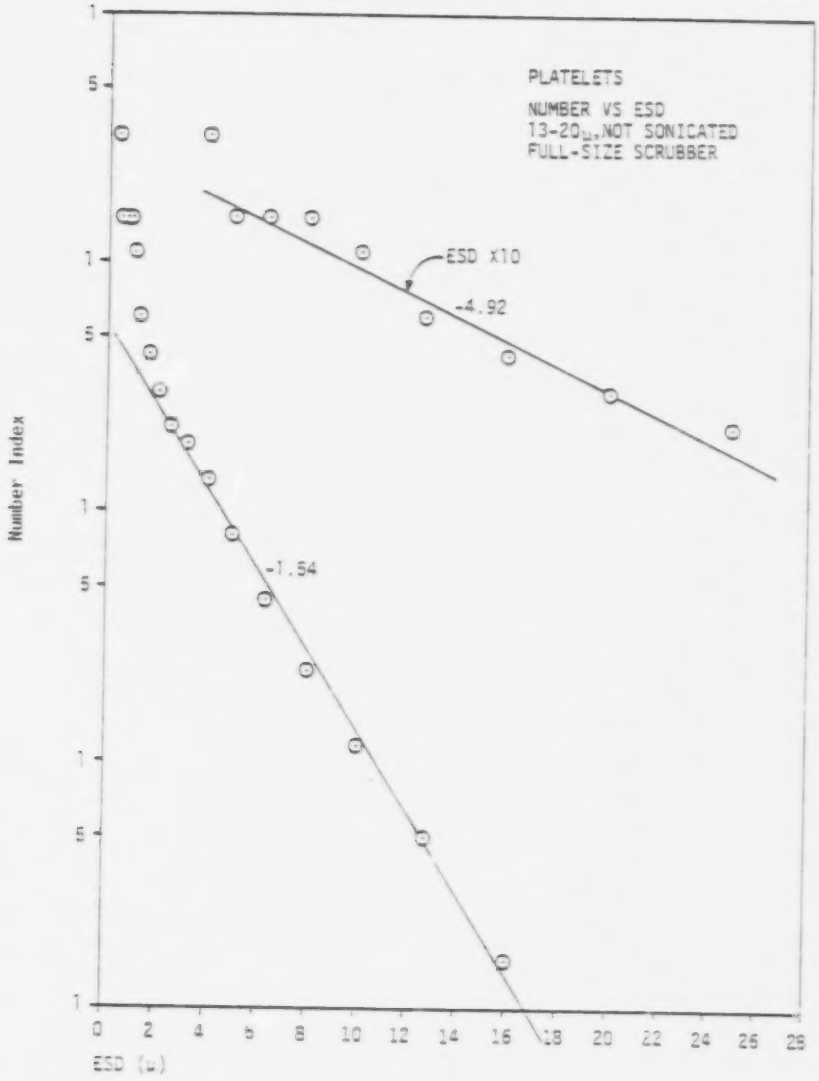

Figure A-10. Logarithmic display of number count calculated from volume count in Figure A-9.

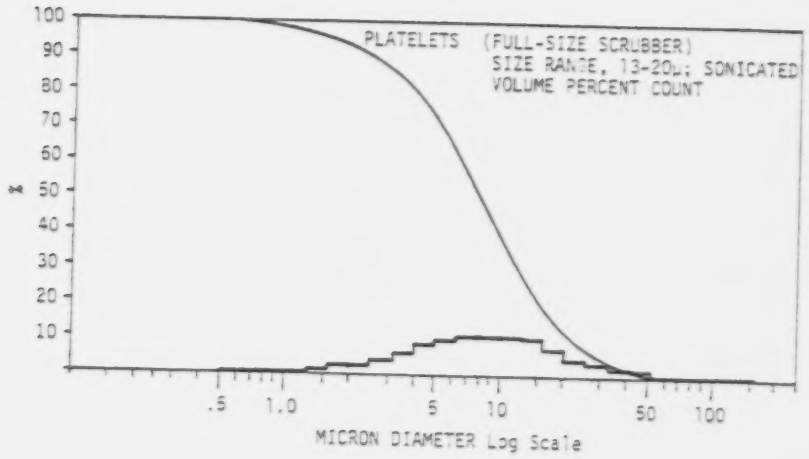

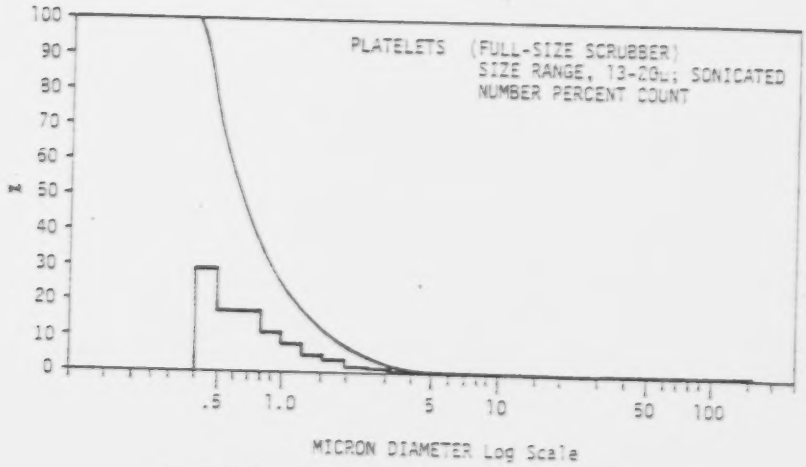

Figure A-11. Platelets in size range 13-20μ; sonicated.
Top: Volume Count
Bottom: Number Count

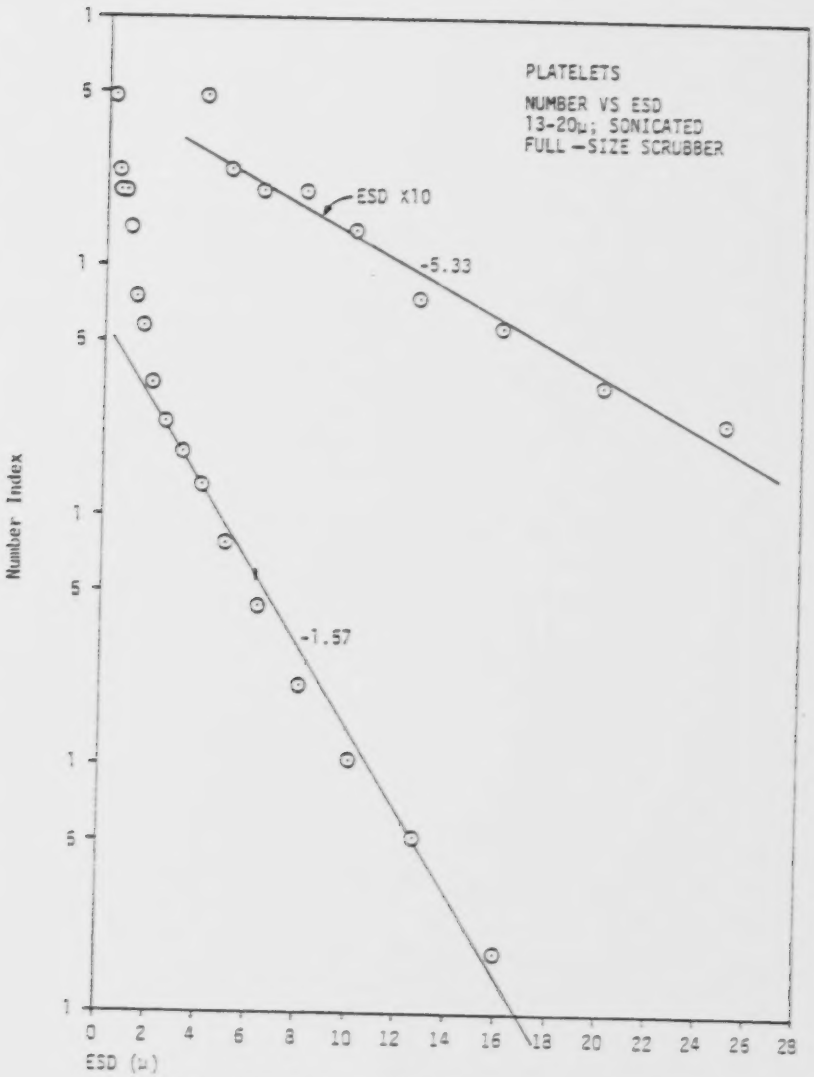

Figure A-12. Logarithmic display of number count in Figure A-11.

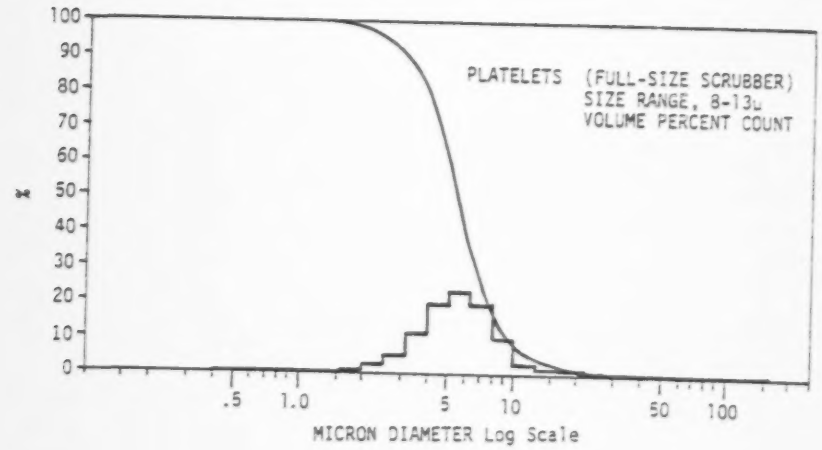

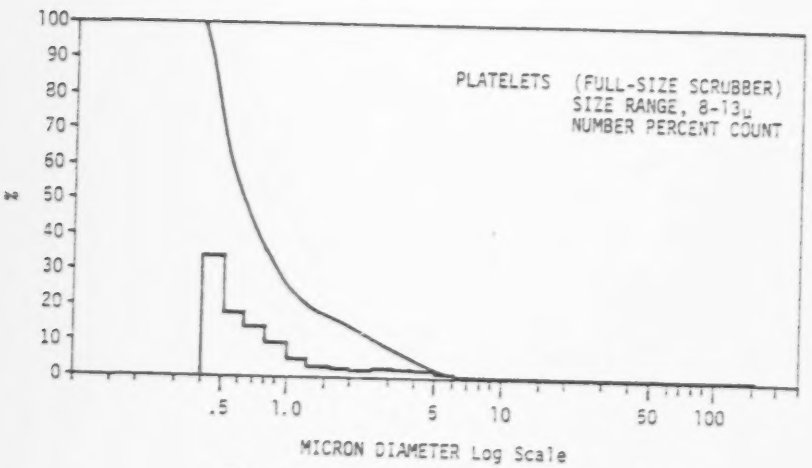

Figure A-13. Platelets in size range 8-13μ.
Top: Volume Count
Bottom: Number Count

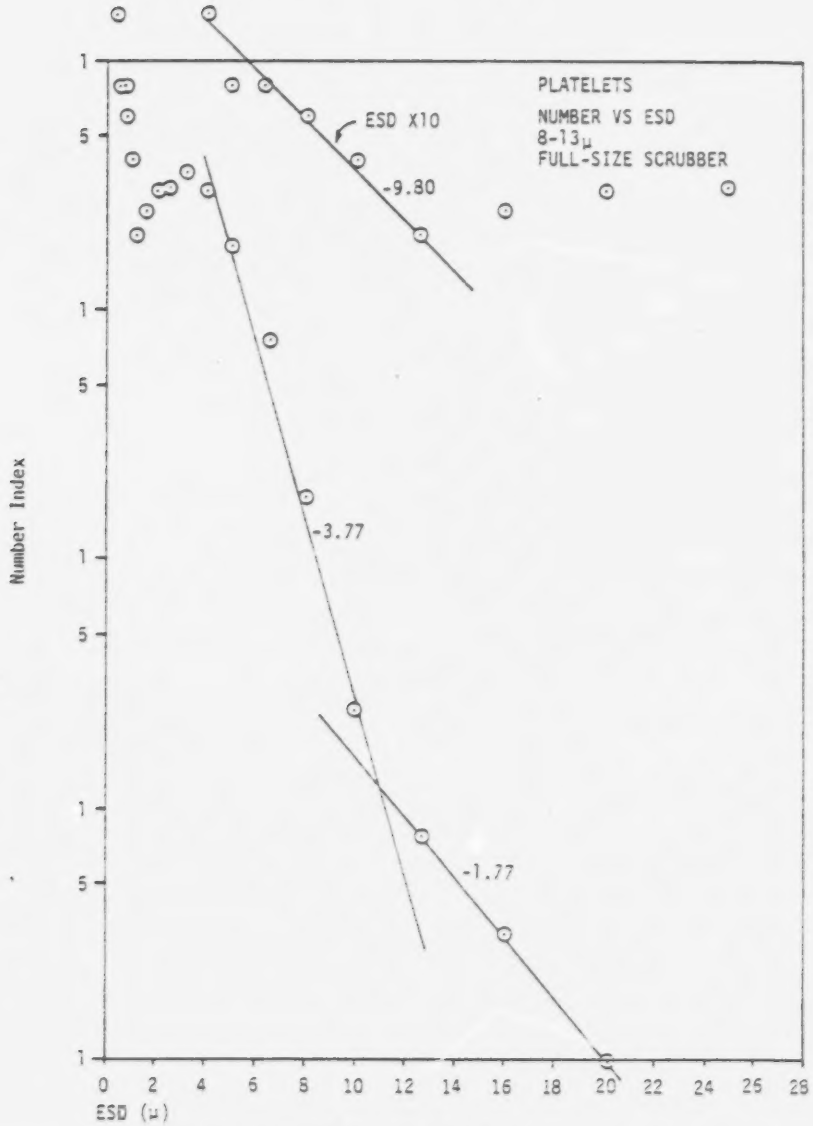

Figure A-14. Logarithmic display of number count in Figure A-13.

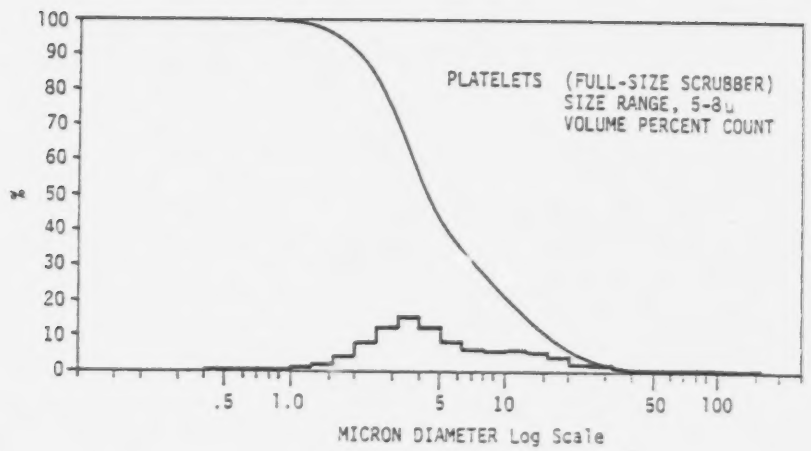

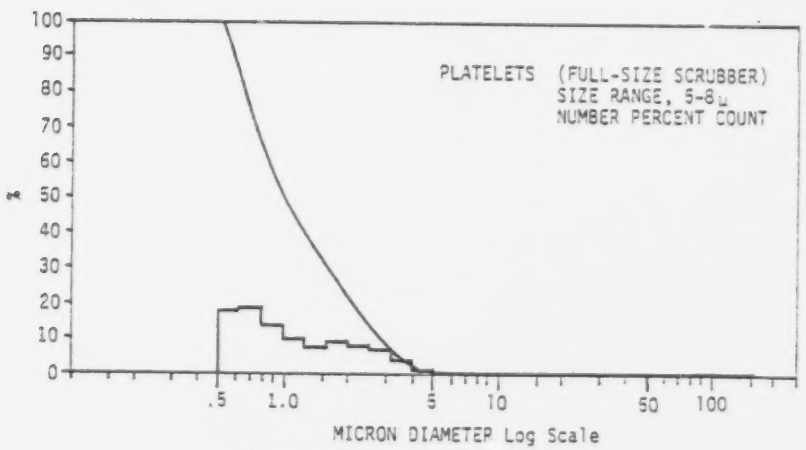

Figure A-15. Platelets in size range 5-8u.
Top: Volume Count
Bottom: Number Count

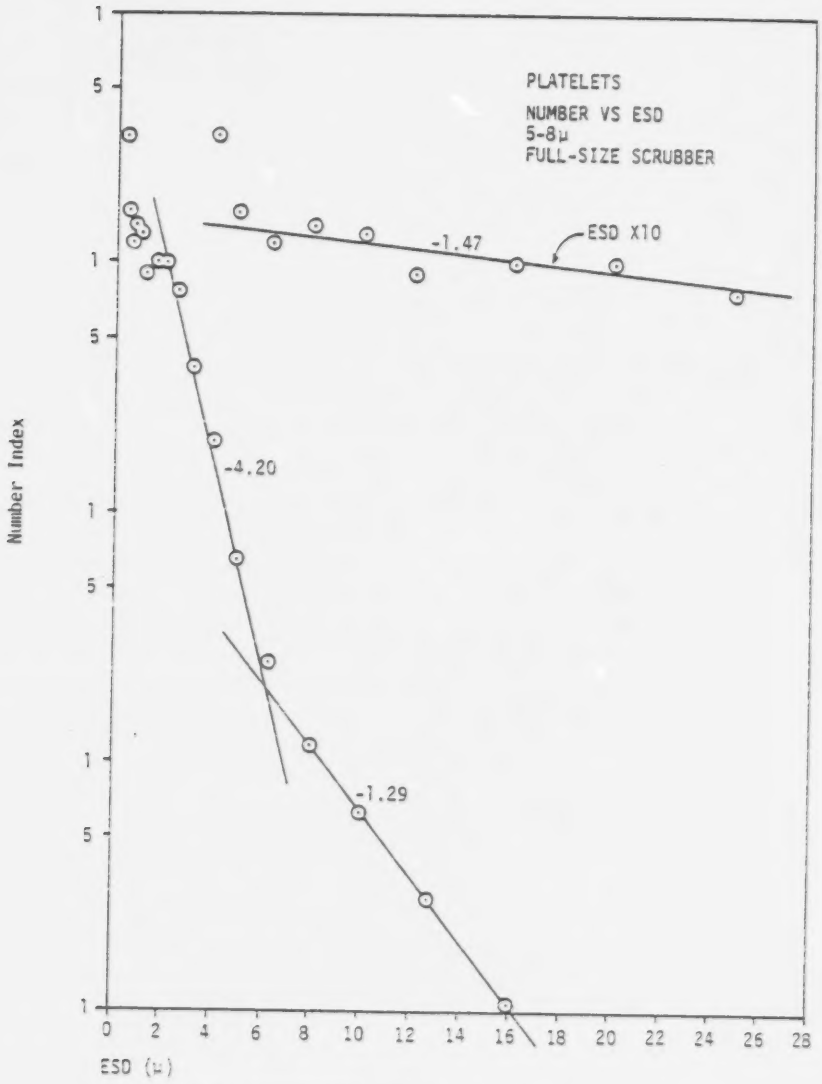

Figure A-16. Logarithmic display of number count in Figure A-15.

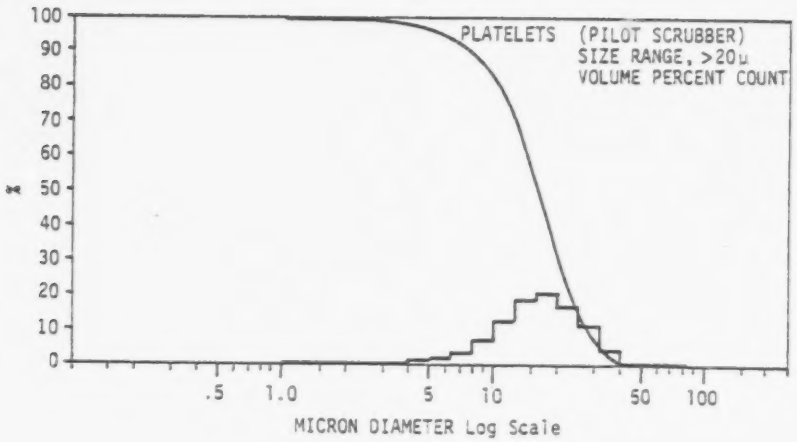

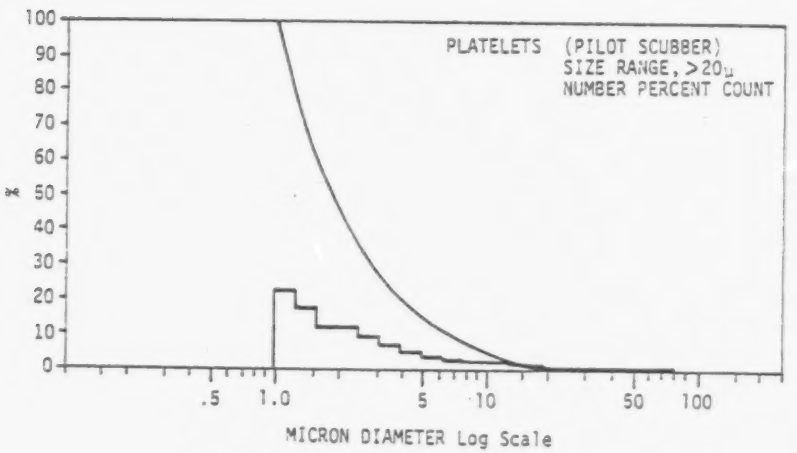

Figure A-17. Platelets in size range >20μ.
Top: Volume Count
Bottom: Number Count

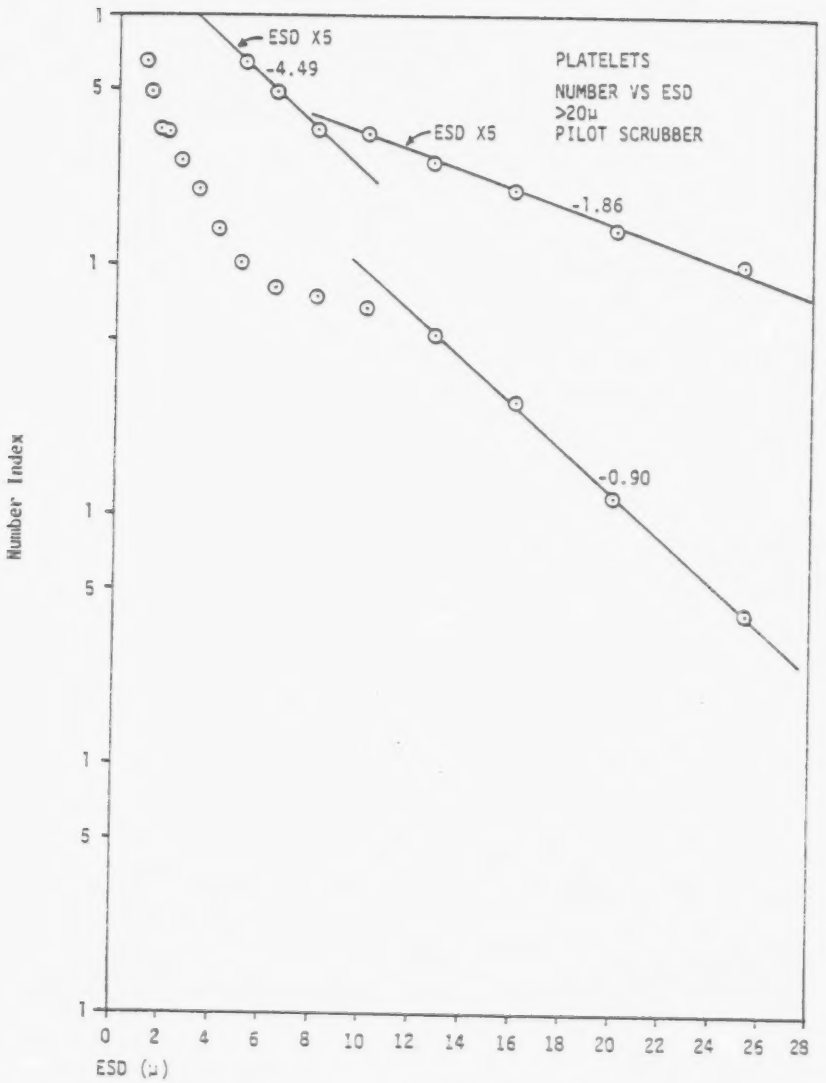

Figure A-18. Logarithmic display of number count in Figure A-17.

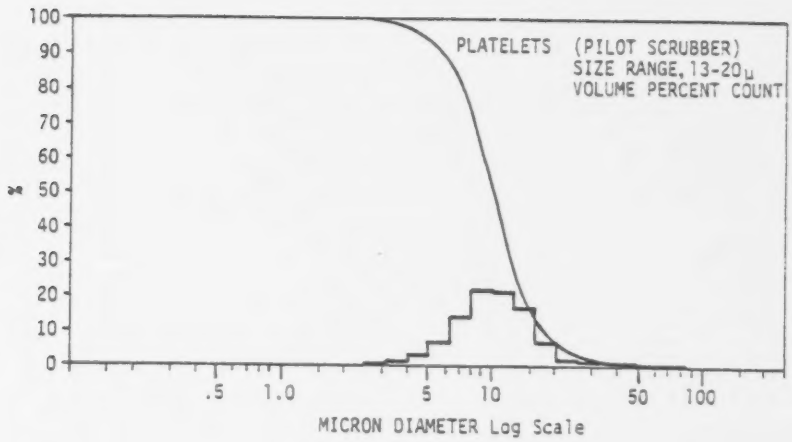

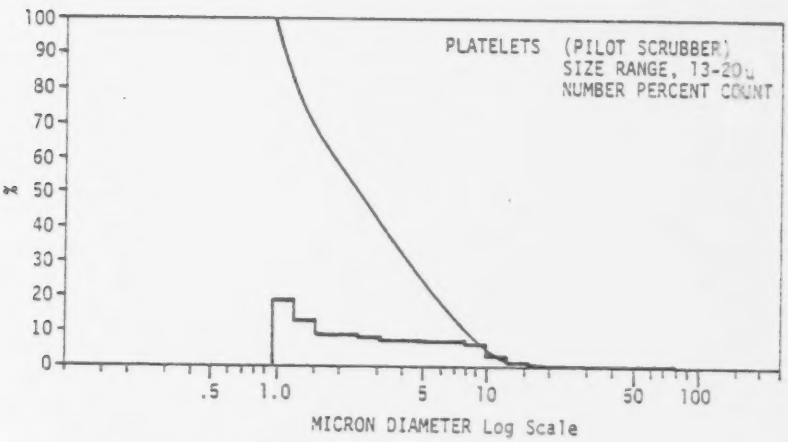

Figure A-19. Platelets in size range 13-20μ; not sonicated.
Top: Volume Count
Bottom: Number Count

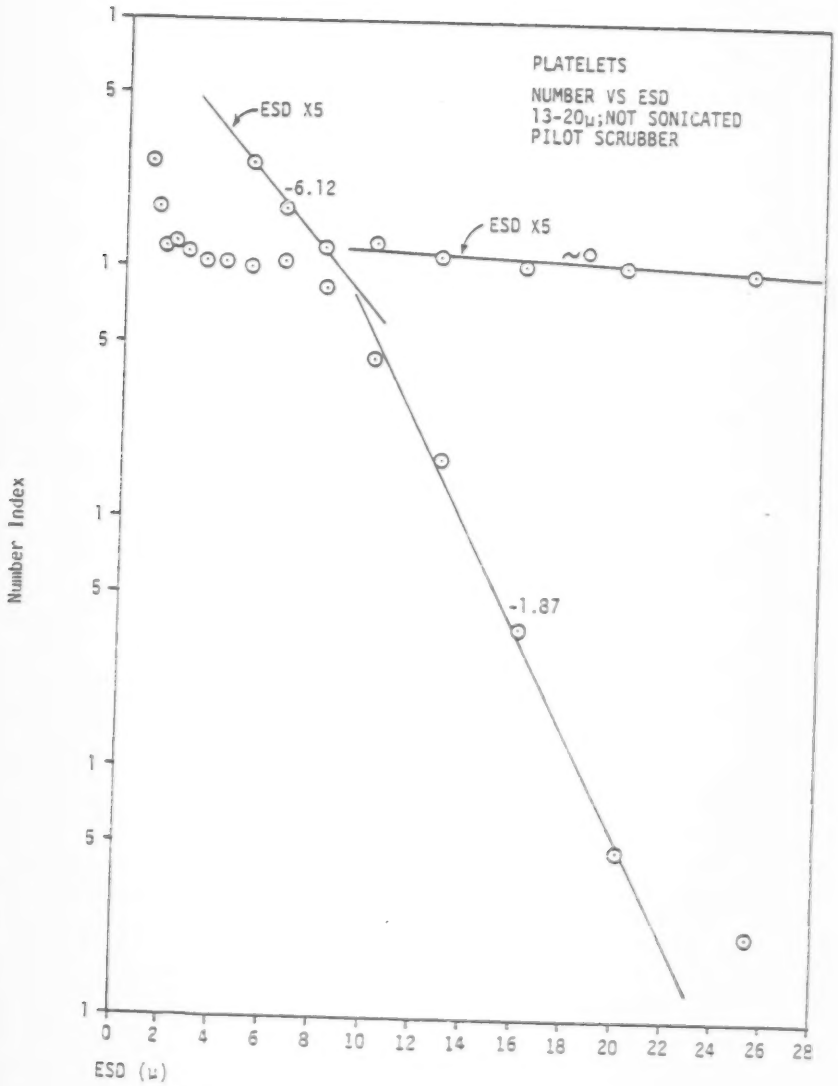

Figure A-20. Logarithmic display of number count in Figure A-19.

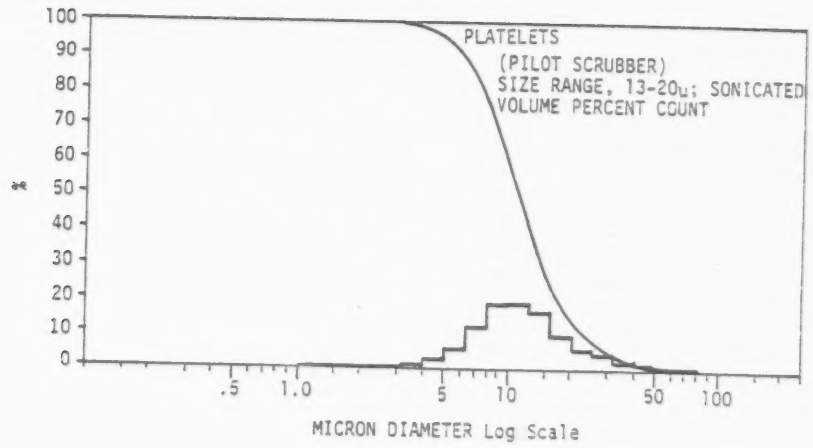

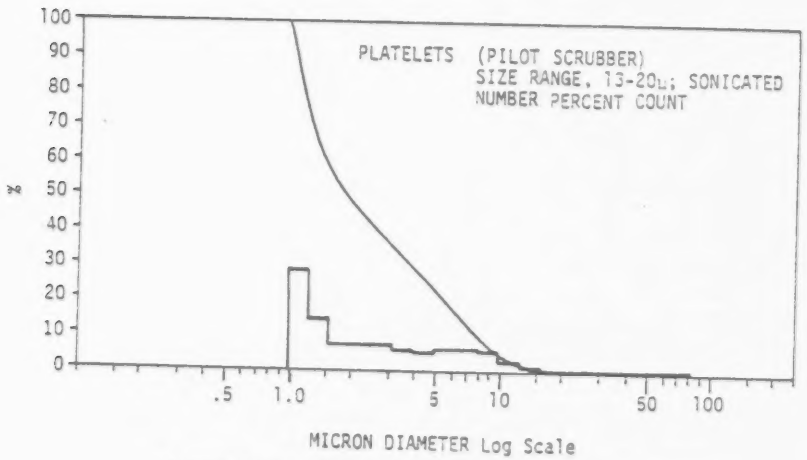

Figure A-21. Platelets in size range 13-20u; sonicated.
Top: Volume Count
Bottom: Number Count

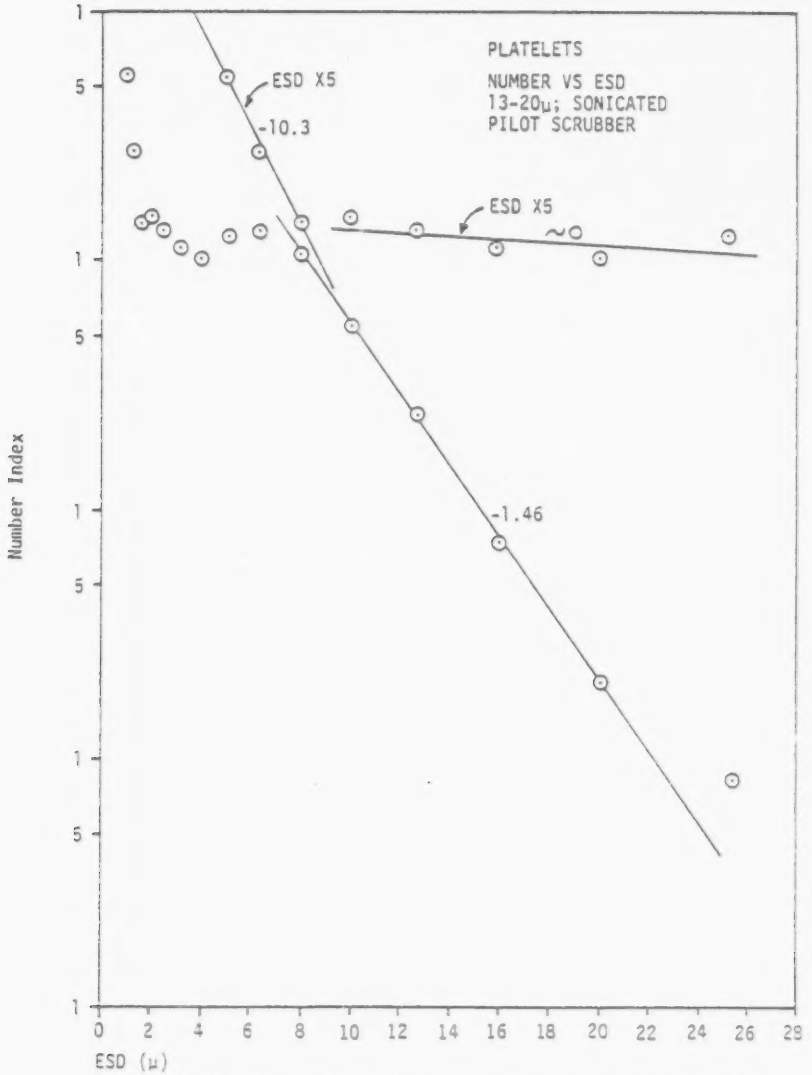

Figure A-22. Logarithmic display of number count in Figure A-21.

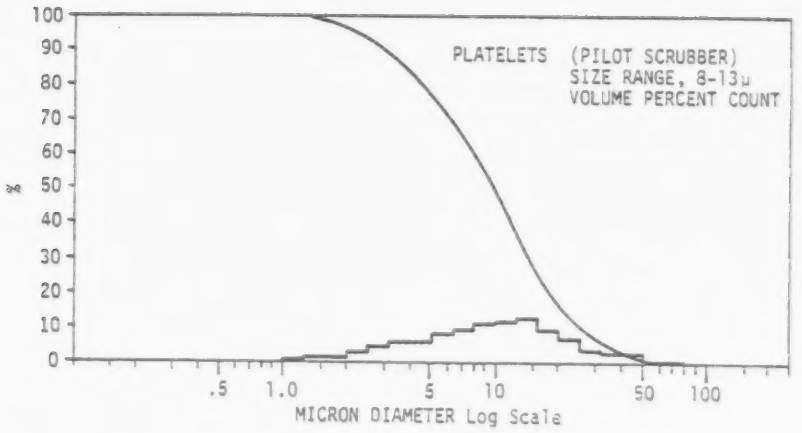

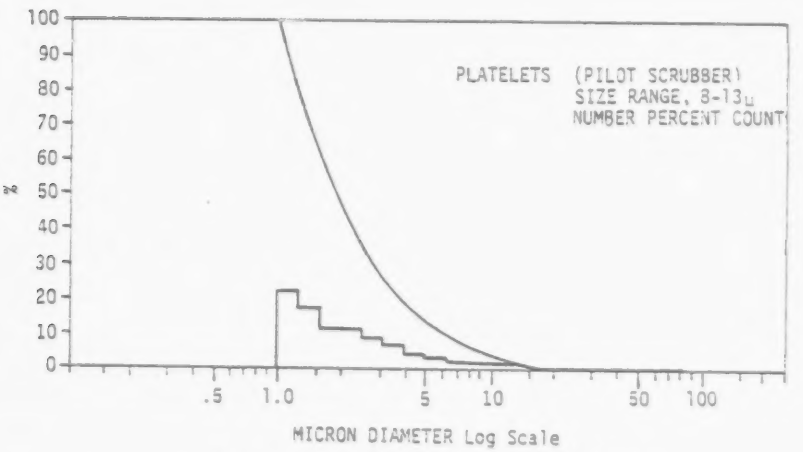

Figure A-23. Platelets in size range 8-13μ.
Top: Volume Count
Bottom: Number Count

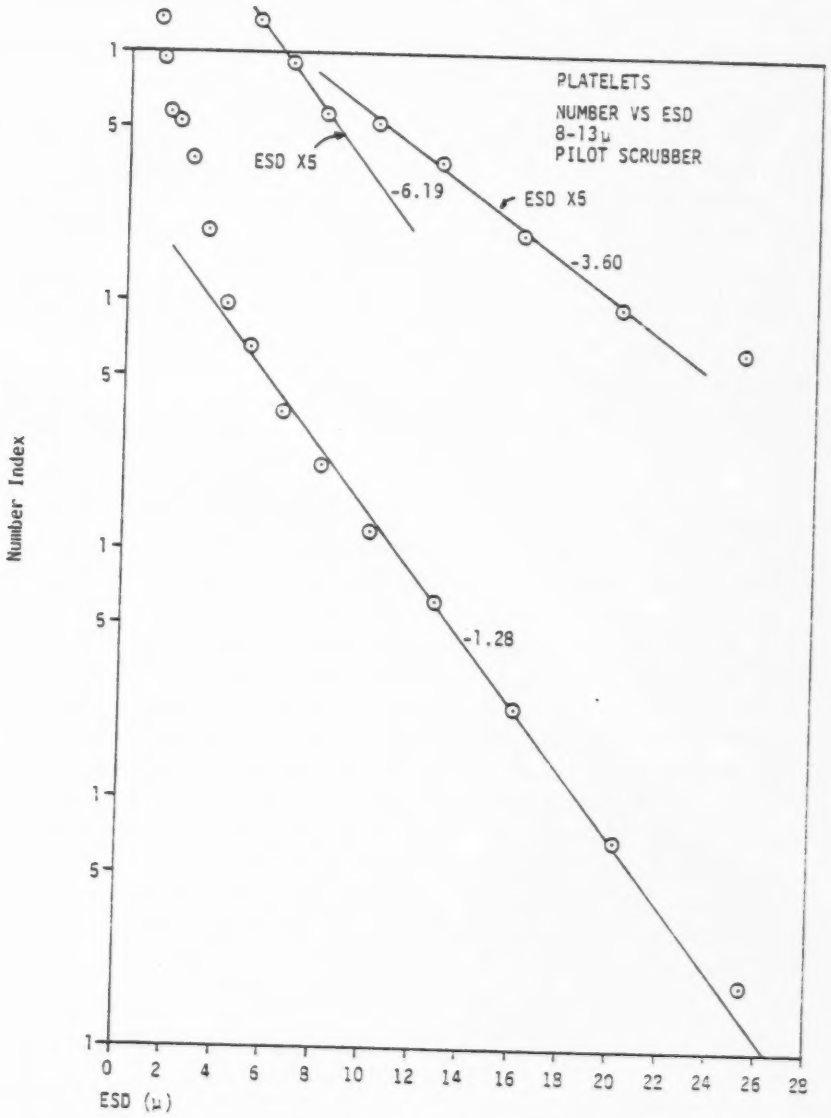

Figure A-24. Logarithmic display of number count in Figure A-23.